200937033A

別紙１

厚生労働科学研究費補助金

地域医療基盤開発推進研究事業

抑肝散の示す精神疾患周辺行動改善に対する科学的検証

平成２１年度　総括研究報告書

研究代表者　遠山正彌

平成２２（２０１０）年　４月

別紙２

研究報告書目次レイアウト（参考）

目　　次

別紙３

厚生労働科学研究費補助金（地域医療基盤開発推進研究事業）
（総括）研究報告書

抑肝散の示す精神疾患周辺行動改善に対する科学的検証に関する研究

研究代表者　：　遠山　正彌

研究要旨
　抑肝散のアルツハイマー病、統合失調症に効能を科学的に解析した。抑肝散の生薬成分であるセンキュウが小胞体ストレスによる神経細胞死を防ぐことによりその作用を発揮すること、その作用はセンキュウより抽出した成分ｘが担っていることを明らかとした。又抑肝散の生薬成分であるチョウトウコウに含まれる成分ｘｘがセロトニン、ドーパミン受容体機能を制御することが明らかとされ、このことが抑肝散の統合失調症に効能を担っていることが解明された。

研究分担者
宮田伸吾
大阪大学大学院医学系研究科・助教
松崎伸介
大阪大学大学院医学系研究科・助教
熊本奈都子
大阪大学大学院医学系研究科・助教
服部剛志
大阪大学大学院医学系研究科・特任助教

A. 研究目的
特定の漢方薬が臨床的に有効で副作用が少ないことは経験的に知られているが「その科学的立証が乏しいため広範囲には使用されていない。漢方薬の効果に科学的根拠が与えられれば上記の問題は解決でき、有効成分の同定から新規創薬の開発に道を開きうる。漢方薬の効能の科学的検証を行い市場に送り出すことはわが国の独自性を国際的にも認知させる絶好の機会である。本研究は臨床的に効果が認められている漢方薬、抑肝散のアルツハイマー病や統合失調症の改善効果を科学的に立証し、抑肝散の作用機序を解明することにある。

B. 研究方法
１）抑肝散のアルツハイマー病への効果の科学的検証
・低酸素、ツニカマイシン、サプシガルジンなどの小胞体ストレスを負荷した培養神経細胞群、　さらに培地に抑肝散を添付した群、　抑肝散を構成する７種の各種生薬をそれぞれ添付した群、抑肝散からセンキュウのみを除いたものを添付した群を用意し細胞死への影響を検討する。
・アルツハイマー病危険遺伝子産物であるプレセニリン１（PS1）変異産物（⊿９）を強制発現させた神経細胞においても同様の群を用意する。
・効果のあった生薬から有効成分を細胞死をマーカーとして抽出する〔近大掛樋教授のグループの協力を得て〕
２）抑肝散の統合失調症への効果の科学的解析〔阪大島田教授のグループの協力を得て〕
D1（Gs）, D2（Gi）, ５HT1A (Gi), ５HT2A (Gq), 5HT2C (Gq), 5HT7 (Gi) 受容体への抑肝散あるいはその構成分の効果を検討した。G 蛋白共役型受容体のうちでも Gi, Gs 共役型受容体はカルシウムイメージングができない。Gi, Gs 共役型受容体と機能的に結合できるキメラ蛋白質を作成しカルシウムイメージングを可能とした、これらの系を用いて抑肝散及びその構成分（本研究ではアルカロイド成分に焦点を絞った）の５ＨＴ、DA 受容体への作用を検討した。
（倫理面への配慮）
なお本研究は培養細胞を使用することから倫理面へのとりたてた配慮は不必要である。

C. 研究成果
１）抑肝散のアルツハイマー病への効果の科学的検証
培養神経細胞に小胞体ストレスを負荷すると一定数の神経細胞が細胞死を起こす。⊿９が強制発現された神経細胞に小胞体ストレスが負荷されると細胞死を起こす細胞数は急増する。すなわちアルツハイマー病における神経細胞死は変異産物が小胞体機能を障害するために引き起こされる。培地に抑肝散を添加するとこれらの神経細胞死が著しく救済された。抑肝散の７種の構成成分のうちセンキュウのみが容量依存性に小胞体ストレス負荷による神経細胞死を救済した。またセンキュウを除いた抑肝散はこのような効果を示さなかった。細胞死を目安としてセンキュウのどの構成分がその効果を担うかを検討したところ成分ｘがその効果を担うこと明らかとした。
２）抑肝酸の統合失調症への効果の科学的解析
抑肝散の構成生薬チョウトウコウに含まれる各種アルカロイドの５HT, DA 受容体への効果を検討した。その結果、成分ｘｘは 5-HT1A 受容体の agonist、5-HT2A, 2C 受容体の antagonist、5-HT7 受容体の antagonist、Ｄ２受容体の partial agonist であることが明らかとなった。他のアルカロイドはこのような効果を有しなかった。

D. 考察

１）抑肝散のアルツハイマー病への効果の科学的検証

抑肝散のアルツハイマー病への効能は神経細胞死を防ぐことにあることが明らかとなった。さらに抑肝散を構成する生薬のうちセンキュウがこの効果を担う主役であり、センキュウに含まれる成分ｘがその作用発現を担っていることも解明できた。今後の大きな課題はどのような機序でセンキュウ、成分ｘが小胞体ストレス負荷による神経細胞死を救済するかである。

２）抑肝酸の統合失調症への効果の科学的解析

抑肝散に含まれる成分 xx が 5HT, DA 受容体を抑制してその効果を発揮することが明らかとなった。

C.　結論

本研究により抑肝散のアルツハイマー病への効能は抑肝散の構成生薬センキュウに含まれる成分ｘが小胞体ストレス負荷による神経細胞死を防ぐことにより発揮されることが明らかとなった。また抑肝散の統合失調症への効能は抑肝散の構成生薬チョウトウコウに含まれるアルカロイド、成分ｘｘ、が５HT, DA 受容体の機能を制御することにより発揮されることも明らかとなった。抑肝散の副作用は極めて弱いことから成分ｘは新規アルツハイマー病治療薬として、成分 xx は新規統合失調症治療薬として期待される。

F. 健康危険情報

特になし。

G. 研究発表

1. 論文発表

1. Okuda H, Kuwahara R, Matsuzaki S, Miyata S, Kumamoto N, Hattori T, Shimizu S, Yamada K, Kawamoto K, Hashimoto R, Takeda M, Katayama T, Tohyama M., Dysbindin regulates the transcriptional level of myristoylated alanine-rich protein kinase C substrate via the interaction with NF-YB in mice brain., 5(1):e8773. (2010)

2. Yamada. K, Matsuzaki S, Hattori T, Kuwahara R, Taniguchi M, Hashimoto H, Shintani N, Baba A, Kumamoto N, Yamada K, Yoshikawa T, Katayama T and Tohyama M., Increased stathmin1 expression in the dentate gyrus causes abnormal axonal arborization., PLoS One., (2010) 5(1) e:8596

3. Matsuzaki S, Hiratsuka T, Kuwahara R, Katayama T, Tohyama M., Caspase-4 is partially cleaved by calpain via the impairment of Ca2+ homeostasis under the ER stress., Neurochem Int., 56(2) (2010) 352-6

4. Katayama T, Hattori T, Yamada K, Matsuzaki S, Tohyama M., The role of the PACAP-PAC1-DISC1 and PACAP-PAC1-stathmin 1 systems in schizophrenia and bipolar disorder: novel treatment mechanisms?., Pharmacogenomics., (2009) 10(12):1967-78.

5. Kubota K, Inoue K, Hashimoto R, Kumamoto N, Kosuga A, Tatsumi M, Kamijima K, Kunugi H, Iwata N, Ozaki N, Takeda M, Tohyama M., Tumor necrosis factor receptor-associated protein 1 regulates cell adhesion and synaptic morphology via modulation of N-cadherin expression., J Neurochem., 110(2009) 496-508.

6. Kousaka A, Mori Y, Koyama Y, Taneda T, Miyata S, and Tohyama M., The distribution and characterization of endogenous PRMT8 in mouse central nervous system., Neuroscience., 163(2009) 1146-57.

7. Kubota K, Kumamoto N, Matsuzaki S, Hashimoto R, Hattori T, Okuda H, Takamura H, Takeda M, Katayama T, Tohyama M., Dysbindin engages in c-Jun N-terminal kinase activity and cytoskeletal organization1., Biochem Biophys Res Commun., 379 (2009) 191-5.

2. 学会発表

ポスター

第 114 回日本解剖学会総会　（岡山）2009. 3. 30

ラット海馬神経細胞樹状突起でのタンパクメチル化酵素の役割

宮田信吾, 森泰丈, 遠山正彌

第 114 回日本解剖学会総会　岡山理科大学 2009. 3. 30.

alphaCaMKII mRNA の樹状突起への局在を決定するタンパク質因子の検索

森泰丈, 宮田信吾, 幸坂葵, 遠山正彌

第 11 回 RNA ミーティング（第 11 回日本 RNA 学会年会）2009. 7. 27-29（新潟）
microRNA による神経細胞成熟化機構の解析
宮田信吾, 橋本亮太, 遠山正彌
第32回日本神経科学学会2009. 9. 16 (名古屋)
演題：DISC1の細胞接着性への影響の検討
服部剛志, 清水尚子, 山田浩平, 桑原　隆亮, 松崎伸介, 片山泰一, 伊藤彰, 遠山正彌
第 32 回日本神経科学大会　2009. 9. 16 (名古屋)
蛋白メチル化による海馬神経細胞樹状突起での局所的翻訳の制御機構
宮田信吾, 森泰丈, 遠山正彌
第 32 回日本神経科学大会　2009. 9. 16（名古屋)
神経細胞における小胞体ストレス応答へのミトコンドリア TRAP1 の関与
嶽本香奈, 宮田信吾, 吉川景子, 片山泰一, 遠山正彌
第 32 回日本神経科学大会　2009. 9. 17.（名古屋)
梢神経再生におけるタンパク質メチル化酵素 PRMT8 の機能解析
幸坂葵, 小山佳久, 森泰丈, 遠山正彌
第115回日本解剖学会総会　（岩手県盛岡市）2010. 3. 28
alphaCaMKII mRNA の樹状突起への輸送を制御するタンパク質群の同定
森泰丈, 宮田信吾, 遠山正彌
第115回日本解剖学会、ポスター発表、2010. 3. 29
演題：統合失調症関連因子DISC1の細胞接着性への検討
服部剛志, 清水尚子, 山田浩平, 桑原隆亮, 松崎伸介, 伊藤彰, 片山泰一, 遠山正彌

国内口頭発表
シンポジウム（国内）
第 114 回日本解剖学会総会　（岡山）2009. 3. 30
ラット海馬神経細胞樹状突起でのタンパクメチル化酵素の役割
宮田信吾、森泰丈、遠山正彌

第 52 回　日本神経化学会大会
2009. 6. 21-24 (群馬)
海馬神経細胞での局所的翻訳における rpS2 の安定化の重要性
宮田信吾、森泰丈、遠山正彌

第 62 回日本自律神経学会総会
2009. 11. 5-6 (和歌山)
精神疾患発症機構への microRNA の関与
宮田信吾、橋本亮太、嶽本香菜、吉川景子、遠山正彌

第 14 回グリア研究会 (大阪) 2009. 11. 14
オリゴデンドロサイト特異的な発現変動因子によるうつ病発症機構の解明
宮田信吾、吉川景子、嶽本香菜、小山佳久、遠山正彌

第 52 回　日本神経化学会大会
2009. 6. 21-24 (群馬)
Alpha CaMKII mRNA の輸送機構に関与するタンパク質の同定
森泰丈、宮田信吾、遠山正彌

第 32 回日本神経化学会－日本生物学的精神医学会 合同シンポジウム
2009. 9. 16-18 (名古屋)
統合失調症関連因子 PACAP による神経分化調節機構の解析
山田　浩平、松崎　伸介、服部　剛志、橋本　均、新谷　紀人、馬場　明道、片山　泰一、遠山　正彌

ワークショップ／シンポジウム（国際学会）
The 9th International Symposium on VIP, PACAP and related peptides 2009. 10. 9.（鹿児島）
Increased stathminl expression in the dentate gyrus of PACAP deficient mice causes abnormal axonal arborizations
Kohei Yamada, Taiichi Katayama, Masaya Tohyama

H. 知的財産権の出願・登録状況（予定を含む。）
１．特許取得
①「漢方薬抑肝散構成生薬のアルツハイマー病神経細胞死抑制とその機序」出願日：2009/3/10

②「抑肝散の統合失調症治療効果とその分子機序」出願日：2009/3/10

２．実用新案登録
３．その他

研究成果の刊行に関する一覧表

雑誌

発表者氏名	論文タイトル名	発表誌名	巻号	ページ	出版年
Okuda H, Kuwahara R, Matsuzaki S, Miyata S, Kumamoto N, Hattori T, Shimizu S, Yamada K, Kawamoto K, Hashimoto R, Takeda M, Katayama T, Tohyama M.	Dysbindin regulates the transcriptional level of myristoylated alanine-rich protein kinase C substrate via the interaction with NF-YB in mice brain.	PLoS One	5(1)	e8773	2010
Yamada. K, Matsuzaki S, Hattori T, Kuwahara R, Taniguchi M, Hashimoto H, Shintani N, Baba A, Kumamoto N, Yamada K, Yoshikawa T, Katayama T and Tohyama M.	Increased stathmin1 expression in the dentate gyrus causes abnormal axonal arborization.	PLoS One	5(1)	e:8596	2010
Matsuzaki S, Hiratsuka T, Kuwahara R, Katayama T, Tohyama M.	Caspase-4 is partially cleaved by calpain via the impairment of Ca2+ homeostasis under the ER stress.	Neurochem Int.	56(2)	352-6	2010
Katayama T, Hattori T, Yamada K, Matsuzaki S, Tohyama M.	The role of the PACAP-PAC1-DISC1 and PACAP-PAC1-stathmin 1 systems in schizophrenia and bipolar disorder: novel treatment mechanisms?.	Pharmacogenomics	10(12)	1967-78	2009
Miyoshi K, Kasahara K, Miyazaki I, Shimizu S, Taniguchi M, Matsuzaki S, Tohyama M, Asanuma M.	Pericentrin, a centrosomal protein related to microcephalic primordial dwarfism, is required for olfactory cilia assembly in mice.	FASEB J.	23(10)	3289-97	2009
Kubota K, Inoue K, Hashimoto R, Kumamoto N, Kosuga A, Tatsumi M, Kamijima K, Kunugi H, Iwata N, Ozaki N, Takeda M, Tohyama M.	Tumor necrosis factor receptor-associated protein 1 regulates cell adhesion and synaptic morphology via modulation of N-cadherin expression.	J Neurochem.	110	496-508	2009
Kousaka A, Mori Y, Koyama Y, Taneda T, Miyata S, and Tohyama M.	The distribution and characterization of endogenous PRMT8 in mouse central nervous system.	Neuroscience	163	1146-57	2009

OPEN ACCESS Freely available online

PLoS one

Dysbindin Regulates the Transcriptional Level of Myristoylated Alanine-Rich Protein Kinase C Substrate *via* the Interaction with NF-YB in Mice Brain

Hiroaki Okuda[1,2☯], Ryusuke Kuwahara[1☯], Shinsuke Matsuzaki[1,3,4☯*], Shingo Miyata[1,3], Natsuko Kumamoto[1], Tsuyoshi Hattori[1,3], Shoko Shimizu[1], Kohei Yamada[1], Keisuke Kawamoto[1], Ryota Hashimoto[3,5], Masatoshi Takeda[5], Taiichi Katayama[4], Masaya Tohyama[1,3,4]

1 Department of Anatomy and Neuroscience, Graduate School of Medicine, Osaka University, Osaka, Japan, **2** Department of Second Anatomy, Faculty of Medicine, Nara Medical University, Nara, Japan, **3** The Osaka-Hamamatsu Joint Research Center for Child Mental Development, Graduate School of Medicine, Osaka University, Osaka, Japan, **4** Department of Child Development and Molecular Brain Science, United Graduate School of Child Development, Osaka University, Kanazawa University and Hamamatsu University School of Medicine, Osaka, Japan, **5** Department of Psychiatry, Osaka University Graduate School of Medicine, Osaka, Japan

Abstract

Background: An accumulating body of evidence suggests that Dtnbp1 (Dysbindin) is a key susceptibility gene for schizophrenia. Using the yeast-two-hybrid screening system, we examined the candidate proteins interacting with Dysbindin and revealed one of these candidates to be the transcription factor NF-YB.

Methods: We employed an immunoprecipitation (IP) assay to demonstrate the Dysbindin-NF-YB interaction. DNA chips were used to screen for altered expression of genes in cells in which Dysbindin or NF-YB was down regulated, while Chromatin IP and Reporter assays were used to confirm the involvement of these genes in transcription of Myristoylated alanine-rich protein kinase C substrate (MARCKS). The sdy mutant mice with a deletion in Dysbindin, which exhibit behavioral abnormalities, and wild-type DBA2J mice were used to investigate MARCKS expression.

Results: We revealed an interaction between Dysbindin and NF-YB. DNA chips showed that MARCKS expression was increased in both Dysbindin knockdown cells and NF-YB knockdown cells, and Chromatin IP revealed interaction of these proteins at the MARCKS promoter region. Reporter assay results suggested functional involvement of the interaction between Dysbindin and NF-YB in MARCKS transcription levels, *via* the CCAAT motif which is a NF-YB binding sequence. MARCKS expression was increased in sdy mutant mice when compared to wild-type mice.

Conclusions: These findings suggest that abnormal expression of MARCKS *via* dysfunction of Dysbindin might cause impairment of neural transmission and abnormal synaptogenesis. Our results should provide new insights into the mechanisms of neuronal development and the pathogenesis of schizophrenia.

Citation: Okuda H, Kuwahara R, Matsuzaki S, Miyata S, Kumamoto N, et al. (2010) Dysbindin Regulates the Transcriptional Level of Myristoylated Alanine-Rich Protein Kinase C Substrate *via* the Interaction with NF-YB in Mice Brain. PLoS ONE 5(1): e8773. doi:10.1371/journal.pone.0008773

Editor: Kenji Hashimoto, Chiba University Center for Forensic Mental Health, Japan

Received November 4, 2009; **Accepted** December 9, 2009; **Published** January 19, 2010

Funding: This work was supported by grants from the Osaka Medical Research Foundation For Incurable Diseases (Shinsuke Matsuzaki) and the Twenty-First Century Center of Excellence (COE) program and the Global COE program (Hiroaki Okuda, Ryusuke Kuwahara, Shinsuke Matsuzaki, Shingo Miyata, Natsuko Kumamoto, Tsuyoshi Hattori, Shoko Shimizu, Kohei Yamada, Taiichi Katayama and Masaya Tohyama). The funders had no role in study design, data collection and analysis, decision to publish, or preparation of the manuscript.

Competing Interests: The authors have declared that no competing interests exist.

* E-mail: s-matsuzaki@anat2.med.osaka-u.ac.jp

☯ These authors contributed equally to this work.

Introduction

Schizophrenia is a common and devastating psychiatric disorder. Lack of patient compliance, due to undesirable side effects and efficacy restricted to positive symptoms, highlights the need to develop novel therapeutics. The etiology of the disease remains unknown, but in recent years a convergence of genetic, pharmacological, and neuroanatomical findings suggest that neural transmission [1–4] and synapse formation [5–11] are involved in schizophrenia. Recent studies suggest that disturbances of Dysbindin (dystrobrevin-binding protein 1; DTNBP1) are involved in this abnormal neural transmission.

The cause of schizophrenia is thought to involve the combined effects of multiple gene components. Genetic linkage and association studies have identified potential susceptibility genes such as Dysbindin [12,13], Neuregulin [14,15], Catechol-*O*-methyltransferase [16–18] and RG4 [19–22]. In particular, it has been reported that chromosome 6p is one of the highest susceptibility regions in linkage studies of schizophrenia [23,24]. Among them, genetic variants in a gene 6p22.3 expressing Dysbindin, which is identified as a protein interacting with dystrobevins [25], have been shown to be strongly associated with schizophrenia [12].

In studies on postmortem brain tissue, decreased levels of Dysbindin protein [26] and mRNA [27] have been shown in

patients with schizophrenia compared with controls. Chronic treatment of mice with antipsychotics did not affect the expression levels of Dysbindin protein and mRNA in their brains [26,28], suggesting that evidence of lower levels of Dysbindin protein and mRNA in the postmortem brains of schizophrenics is not likely to be a simple artifact of antemortem drug treatment. In addition, previous reports have shown that diverse high-risk single nucleotide polymorphisms (SNPs) and haplotypes could influence Dysbindin mRNA expression [27,29]. These data indicate that the Dysbindin gene may confer susceptibility to schizophrenia through reduced Dysbindin expression.

Several lines of evidence suggest that Dysbindin may be associated with brain function. SNPs in *Dysbindin* have been associated with intermediate cognitive phenotypes related to schizophrenia such as IQ and working and episodic memory, and a Dysbindin haplotype has been associated with higher educational attainment [30,31]. In addition, several reports suggest the involvement of Dysbindin in cognitive functions [32–34]. These findings strongly suggest the importance of Dysbindin in brain function. At the cellular level, Dysbindin is located at both pre- and post-synaptic terminals [26,35], and is thought to be involved in postsynaptic density (PSD) function and the trafficking of receptors (NMDA, GABAergic, and nicotinic). Over-expression of Dysbindin increases glutamate release from pyramidal neurons in cell culture, possibly because of its role in vesicular trafficking [36]. Decreases in Dysbindin mRNA and protein levels have been reported in regions previously implicated in schizophrenia: the prefrontal cortex, midbrain, and hippocampus [26,27]. However, the molecular mechanisms of how decreases in Dysbindin expression may contribute to vulnerability to schizophrenia remain unknown.

Thus, we examined the interacting partners of Dysbindin using yeast two-hybrid analysis in order to help elucidate the function of Dysbindin. These interacting-protein data suggest that Dysbindin is involved in such processes as neurotransmission, cell signaling, the cytoskeleton and transcription. (Matsuzaki S *et al.* in submission). In addition, our previous reports suggest the following; (1) decreased expression of Dysbindin might increase dopamine release in the brain resulting in the observed abnormal behavior in sdy mice (Dysbindin KO mice) [37,38], (2) Dysbindin is likely involved in dopaminergic or glutamatergic transmission [36,39], (3) Dysbindin is likely involved in neurotransmission by binding with the BLOC1 complex, and with transcription by binding with transcription-related genes (Matsuzaki S *et al.* in submission), (4) the expression level of Dysbindin may affect the expression of SNAP25 [36,39], (5) Dysbindin may play a key role in coordinating JNK signaling and actin cytoskeleton required for neural development [40]. These findings suggest that Dysbindin may influence neurotransmission and neural development *via* interaction with other factors or by regulation of transcription.

In a previous paper, we identified several Dysbindin interacting partners including the transcription factor, nuclear transcription factor Y beta (NF-YB) (Matsuzaki S *et al.* in submission). NF-YB belongs to a family of CCAAT-binding transcription factors, which are important for the basal transcription of a class of regulatory genes and are involved in cellular reactions [41–44]. Subsequently, in this study, we examined the functional involvement of Dysbindin in transcription *via* its interaction with NF-YB. As a result, we showed that the NF-YB/Dysbindin complex regulates the transcription of MARCKS *via* interaction with certain CCAAT sequences, and abnormal NF-YB/Dysbindin interaction could cause alterations such as impaired neural transmission and abnormal development of neurons.

Results

Dysbindin Exists within the Nucleus in Addition to the Cytoplasm

We examined the existence of Dysbindin in the nucleus, because Dysbindin should exist within the nucleus to play a functional role in transcriptional regulation. We used an overexpression vector for Dysbindin tagged with -FLAG or -V5 to check the intracellular localization of Dysbindin. The fractionation study using Dysbindin-FLAG-overexpressing HEK293 cells shows that Dysbindin exists mainly in the cytosol while a small amount exists in the nucleus (Figure 1A), and Dysbindin-V5 showed the same results (data not shown). These results are in accordance with a previous report [45]. Morphologically, Dysbindin is localized mainly in the cytoplasm with a perinuclear high density region in HEK293 cells and SY5Y cells; however, a faint immunoreaction was also seen within the nucleus (Figure 1B -a and -b). Furthermore, pretreatment with leptomycine-B (LPB), which inhibits export from the nucleus to the cytoplasm, caused a slight Dysbindin increase in cells, which then showed nuclear localization of Dysbindin (Figure 1B -c and -d). These findings suggest that Dysbindin protein is shuttled between the nucleus and the cytoplasm.

Dysbindin Binds to the Transcription Factor NF-YB

Using yeast two-hybrid screening, we identified several transcriptional factors as candidates that may interact with Dysbindin. We selected NF-YB, one of the candidates, and confirmed a Dysbindin-NF-YB interaction by immunoprecipitation assay using HEK293T cells which express NF-YB endogenously (Figure 1A). HEK293T cells were transfected with expression vectors for Dysbindin-V5, and cell lysates were subjected to immunoprecipitation with anti-V5 or anti-NF-YB antibodies, followed by Western blot analysis with a reciprocal antibody. NF-YB was detected in the immunoprecipitates with an anti-V5 body, comparing to the immunoprecipitates with control IgG (Figure 2A), while Dysbindin-V5 was detected in the immunoprecipitates with an anti-NF-YB antibody, comparing to control IgG (data not shown). Thus, Dysbindin and NF-YB are physiologically associated with each other in transfected mammalian cells.

To further our research, we produced a specific anti-Dysbindin antibody with high titer. The antibody detects endogenous Dysbindin in cell and mouse brain samples, though it did not detect any bands corresponding to Dysbindin from the lysates of

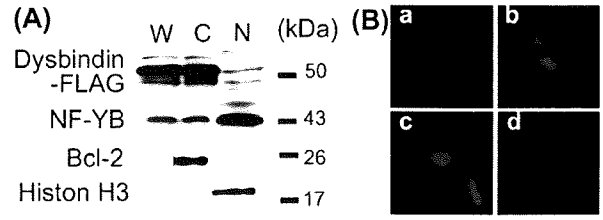

Figure 1. The nuclear localization of Dysbindin. (A) HEK293 cells overexpressing Dysbindin-FLAG were separated into nuclear and cytosolic fractions. Anti-Bcl2 antibody was used for the cytosolic fraction marker and anti-Histone H3 antibody was used for the nuclear fraction marker. W: Whole cell lysates, N: Nuclear Fraction, C: Cytosolic fraction. Dysbindin-FLAG was slightly present in the nuclear fraction. (B) Dysbindin-GFP was overexpressed in HEK293 cells (a and c) or in SH-SY5Y cells (b and d). Dysbindin was usually localized in the cytoplasm and slightly in the nucleus (a and b). After treatment with LMB, a potent inhibitor of CRM1-dependent nuclear export, Dysbindin-GFP accumulated in the nucleus (c and d).
doi:10.1371/journal.pone.0008773.g001

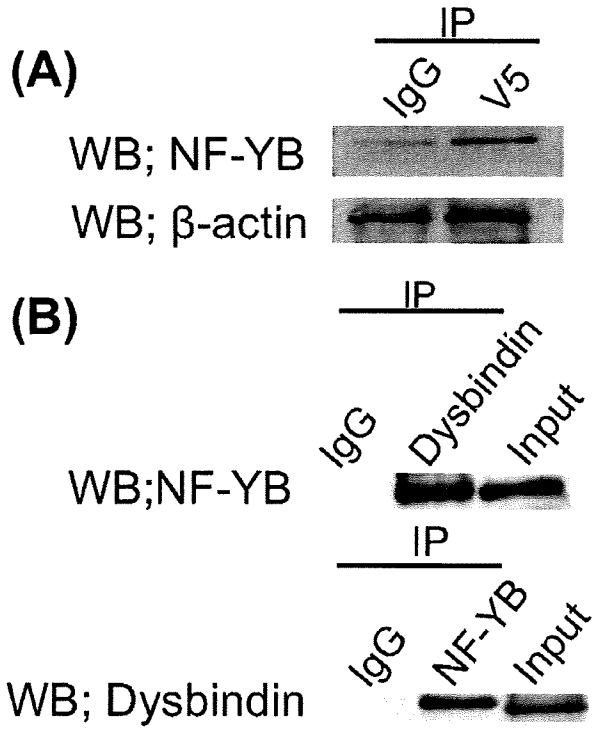

Figure 2. The interaction between Dysbindin and NF-YB. (A) HEK293 cells were transfected with Dysbindin-V5. Immunoprecipitates (IP) of lysates of HEK293 cells expressing Dysbindin-V5 obtained by antibodies to tag proteins (V5) (2nd lane), or nonspecific rabbit IgG (IgG) (1st lane) were subjected to Western blot with anti- NF-YB antibody (upper panel). Dilutions of the lysate (5%, HEK293 cells) were subjected to Western blot with anti-β-actin antibody (lower panel). (**B**) Immunoprecipitates (IP) of lysates of SH-SY5Y cells obtained by antibodies to Dysbindin (upper panel 2nd lane), NF-YB (lower panel 2nd lane), or nonspecific rabbit IgG (IgG) (1st lane of both panels) were subjected to Western blot with anti- NF-YB antibody (upper panel) or Dysbindin antibody (lower panel). Dilutions of the lysate (5%, HEK293 cells) were subjected to Western blot with anti-NF-YB antibody (3rd lane of upper panel) or Dysbindin antibody (3rd lane of lower panel).
doi:10.1371/journal.pone.0008773.g002

Dysbindin knockout mouse brain [40]. The existence of endogenous Dysbindin and endogenous NF-YB in lysates from SH-SY5Y cells was confirmed by Western Blot (Figure 2B, 3rd lane of both panels). Immunoprecipitation using the lysates with antibodies for Dysbindin and NF-YB and subsequent Western blot revealed the interaction of endogenous Dysbindin with endogenous NF-YB (Figure 2B, 2nd lane of both panels), and this binding was also confirmed using adult mouse brain lysates (data not shown).

Downregulation of Dysbindin Causes Upregulation in Expression Levels of Myristoylated Alanine-Rich Protein Kinase C Substrate (MARCKS)

As shown above, we had revealed an interaction between Dysbindin and NF-YB. This result suggests that Dysbindin may be functionally involved in transcription of some genes regulated by NF-YB. We screened for genes displaying altered expression by means of a DNA chip, using RNA extracts from the Dysbindin or NF-YB knockdown human neural cell line, SH-SY5Y. The expression of either *Dysbindin* or *NF-YB* was decreased by the corresponding siRNA for each gene, and the effects of siRNA on Dysbindin or NF-YB were confirmed by Western blot analysis (Figure S1). The genes showing increased expression in the Dysbindin knockdown cells, as well as in the NF-YB knockdown cells, are listed in Table 1A, while those showing decreased expression are listed in Table 1B. Next, using the DANASIS 2.0 system or sequencing of the promoter region, we screened for genes having the CCAAT sequence in the promoter region, because NF-YB is known to bind with high specificity to the CCAAT motif in the promoter region of a variety of genes (Table 1, gene names shown in red). We then focused on three genes; Myristoylated alanine-rich protein kinase C substrate (*MARCKS*) [46–48], Phospholipase C beta 4 (*PLCB4*) [49] and Synaptotagmin 1 (*SYT1*) [50], because an accumulating number of reports point to the involvement of impaired neural transmission in the schizo-

Table 1. The list of genes altered by Dysbindin as well as NF-YB.

(A) Upregulated genes				
Dysbindin		NF-YB		
2 h	24 h	2 h	24 h	Gene name
1.343	1.393	1.234	1.409	"Chaperonin containing TCP1, subunit 4 (delta)"
1.344	1.325	1.232	1.352	BCL2-associated athanogene
1.296	1.406	1.485	1.394	***Thymine-DNA glycosylase***
1.315	1.476	1.261	1.295	***Myristoylated alanine-rich protein kinase C substrate***
1.355	1.559	1.430	1.434	Homer homolog 3 (Drosophila)
1.411	1.400	1.368	1.224	Hypothetical protein MGC2749
1.238	2.037	1.368	1.259	***Secretogranin II (chromograninC)***
(B) Decreased genes				
Dysbindin		NF-YB		
2 h	24 h	2 h	24 h	Gene name
0.768	0.701	0.762	0.642	***Brain protein 44-like***
0.747	0.649	0.757	0.677	***Jun dimerization protein 2***
0.827	0.643	0.805	0.803	Kinesin family member 3A
0.734	0.790	0.764	0.601	Sarcosine dehydrogenase
0.814	0.698	0.762	0.722	***Phospholipase C, beta 4"***
0.761	0.645	0.670	0.699	***Synaptotagmin I***
0.815	0.518	0.741	0.780	B cell RAG associated protein
0.729	0.634	0.790	0.796	Hypothetical protein FLJ39370
0.763	0.631	0.760	0.668	SEC63-like (S. cerevisiae)
0.813	0.776	0.824	0.811	***ADP-ribosylation-like factor 6 interacting protein 5***
0.732	0.588	0.608	0.749	***Prothymosin, alpha (gene sequence 28)"***
0.693	0.645	0.769	0.787	***Homeodomain interacting protein kinase 3***
0.710	0.711	0.744	0.618	Similar to AV028368 protein
0.772	0.759	0.762	0.682	***Tropomyosin 4***
0.833	0.651	0.819	0.753	Lactate dehydrogenase A

(A) The genes upregulated by the knockdown of Dysbindin that were in common with those upregulated by the knockdown of NF-YB are listed. The genes showed by bold and italic format have the CCAAT motif.
(B) The genes downregulated by the knockdown of Dysbindin that were in common with those downregulated by the knockdown of NF-YB are listed. The genes showed by bold and italic format have the CCAAT motif.
doi:10.1371/journal.pone.0008773.t001

phrenia pathology. In addition, we considered the involvement of the genes in psychiatric diseases and we narrow down to MARCKS [51] and SYT1 [52]. Interestingly, a previous report suggests the alteration of SYT1 in schizophrenia patients [52]. The paper shows increase of SYT1 mRNA in younger schizophrenia patients group, while it shows decrease of SYT1 mRNA in older schizophrenia patients. These results suggest the complicated and multiple regulation of SYT1 transcriptional regulation. Thus, we examined the functional involvement of the Dysbindin-NF-YB interaction in *MARCKS* transcription.

To confirm the involvement of the knockdown of Dysbindin or NF-YB in the upregulation of MARCKS, we performed Western blot analysis using Dysbindin or NF-YB knockdown SH-SY5Ycells. Comparing the expression level of the MARCKS protein with that of control cells, Dysbindin knockdown cells showed upregulation of MARCKS protein (Figure 3A). To confirm the effect of Dysbindin on MARCKS *in vivo*, we examined the expression of MARCKS protein in the hippocampus with advancing age of the Dysbindin knockout mice, comparing with that found in wild-type mice. In the wild-type mice, a peak in MARCKS protein expression in the hippocampus was identified at postnatal day 15 and 20 (Figure 3B), and then decreased markedly over time. However, such a decrease was not observed in the Dysbindin knockout mice, where large amounts of Dysbindin protein were still expressed in the hippocampii of older mice (Figure 3B). These findings suggest that downregulation of Dysbindin may enhance transcription of the *MARCKS* gene, resulting in the upregulation of MARCKS protein.

We performed chromatin IP analysis using SH-SY5Y cells over-expressing Dysbindin-Flag, to explore the possibility that the Dysbindin-NF-YB complex could affect the transcription of *MARCKS via* interaction with the promoter region of *MARCKS*. The cells were stimulated by retinoic acid to induce *MARCKS*, and were collected as the samples for chromatin IP. PCR products from the chromatin IPs suggest that Dysbindin and NF-YB simultaneously interact with the promoter region of *MARCKS*, but control IgG experiments did not show this result (Figure 3C). These findings indicate that the Dysbindin-NF-YB complex interacts with the promoter region of the *MARCKS* gene resulting in inhibition of *MARCKS* transcription.

The Transcriptional Level of the *MARCKS* Gene Is Regulated by Dysbindin *via* the NF-YB Binding Motif, CCAAT-2

As shown in Figure 4A, the 5′−UTR region of the *MARCKS* gene has two kinds of CCAAT sequences; one CCAAT motif located between UTR −1152 and −700 and the other located between UTR −700 and −614. In this study, we tentatively named the former CCAAT sequence "CCAAT-1" and the latter "CCAAT-2." It is well known that NF-YB binds to the CCAAT motif to regulate transcription of target genes. Thus, we examined whether CCAAT motifs are essential to the regulation of *MARCKS* transcription by means of a luciferase assay, using the following five vectors containing shorter RNA probes; UTR(1152)-Luc, UTR (953)-Luc, UTR(700)-Luc, UTR(614)-Luc, and UTR(462)-Luc (Figure 4A). These constructs were transiently transfected into SH-SY5Y cells which express Dysbindin and NF-YB endogenously, and luciferase activity in each cell line was measured 24 hours after stimulation with retinoic acid. As baseline, we used luciferase activity detected in the SH-SY5Y cells expressing the UTR(1152)-Luc after retinoic acid stimulation (Figure 4A). In the cells transfected with UTR (953)-Luc containing both CCAAT sequences and UTR(700)-Luc containing the CCAAT-1 sequence but lacking the CCAAT-2 sequence, luciferase activity remained at baseline level after stimulation with retinoic acid (Figure 4A). However, luciferase activity was markedly increased in the cells expressing UTR(614)-Luc after retinoic acid stimulation (Figure 4A). These results suggest that the CCAAT-2 motif plays an important role in inhibition of *MARCKS* transcription. Furthermore, the SH-SY5Y cells transfected with UTR(462)-Luc lacking CCAAT-1, CCAAT-2 and the Sp1 region showed very low luciferase activity (Figure 4A), indicating that Sp1 is indispensable for *MARCKS* transcription.

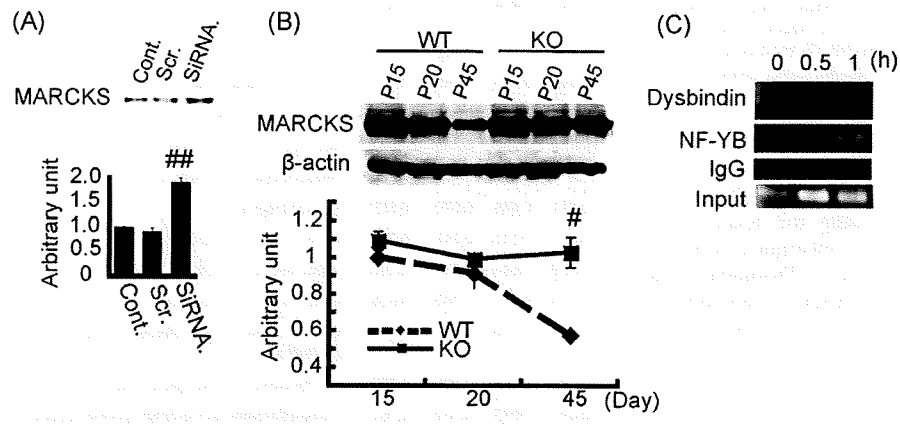

Figure 3. The effects of Dysbindin on MARCKS expression levels. (A) SH-SY5Y cells were transfected with scrambled siRNA or siRNA for Dysbindin. Cell lysate of non-treated cells (Cont.), scrambled RNAi-transfected cells (Scr.) and RNAi for Dysbindin-transfected cells (siRNA) were subjected to Western blot with anti-MARCKS antibody. Columns and vertical bars denote the means ± SEM (triplicate independent experiments). Dysbindin knockdown cells exhibited significant reduction of MARCKS expression compared with control cells ($P<0.001$, Student's t-test). (B) Hippocampus lysates were collected from wild-type mice or Dysbindin KO mice at P15, P20 and P45. The lysates were subjected to Western blot with anti-MARCKS antibody. Graphs and vertical bars denote the means ± SEM (triplicate independent experiments). At P45, Wild-type mice showed significant decreased MARCKS expression, while Dysbindin KO mice showed a maintained MARCKS expression. These data were confirmed by triplicate independent experiments ($P<0.01$, Student's t-test). (**C**)Chromatin IP (ChIP) was performed using SH-SY5Y cells under the stimulation of retinoic acid. The promoter region of *MARCKS* was detected both in the IPs of anti-Dysbindin antibody (1st panel) and those of anti-NF-YB antibody (2nd panel), but not in the IPs of IgG (3rd panel).
doi:10.1371/journal.pone.0008773.g003

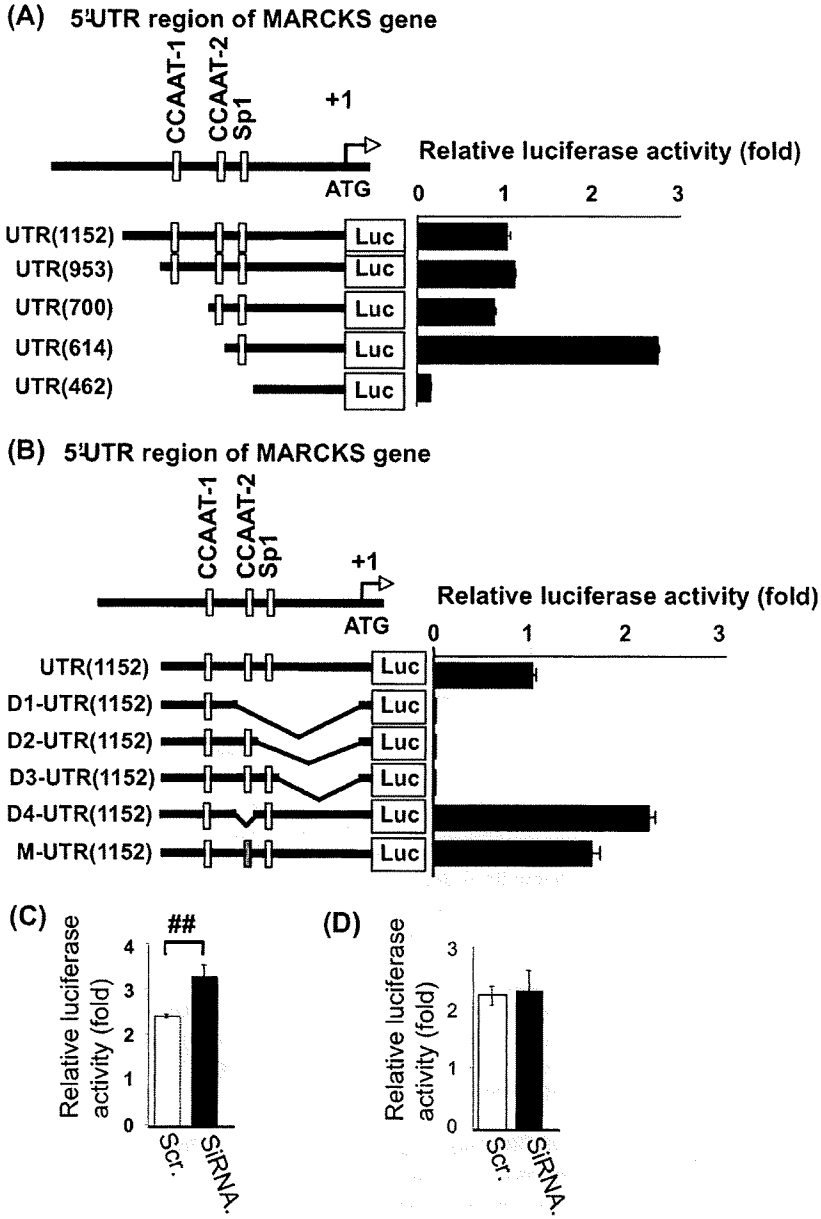

Figure 4. Dysbindin regulates the transcription of MARCKS via the CCAAT2 sequence. (A) The following five vectors were used for luciferase assay, containing shorter DNA probes; UTR(1152)-Luc, UTR (953)-Luc, UTR(700)-Luc, UTR(614)-Luc, and UTR(462)-Luc, were transfected into SH-SY5Y cells and Luciferase activity was measured. UTR(614), which lacks CCAAT1, showed increased luciferase activity. The luciferase activity of UTR(1152) was used as control. Columns and vertical bars denote the means ± SEM (triplicate independent experiments). (B) UTR(1152)-Luc vector and deleted or point mutation of UTR(1152)-Luc vectors, [D1-UTR(1152)-Luc], [D2-UTR(1152)-Luc], [D3-UTR(1152)-Luc] [D4-UTR(1152)-Luc] and [M-UTR(1152)-Luc], were transfected into SH-SY5Y cells and Luciferase activity was measured. [D4-UTR(1152)-Luc], which lacks CCAAT2, and [M-UTR(1152)-Luc], which has a point mutation in the CCAAT2 sequence, showed increased luciferase activity. The luciferase activity of UTR(1152) was used as the control. Columns and vertical bars denote the means ± SEM (triplicate independent experiments). (C and D) Scrambled RNAi-transfected SH-SY5Y cells and Dysbindin RNAi-transfected SH-SY5Y cells were transfected with the UTR(1152)-Luc vector (C) or D4-UTR(1152)-Luc (D) and Luciferase activity was measured. UTR(1152)-Luc vector-expressing cells showed the effect of Dysbindin expression levels on luciferase activity, but D4-UTR(1152)-Luc expressing cells did not. Columns and vertical bars denote the means ± SEM (triplicate independent experiments; $P<0.001$, Student's t-test).
doi:10.1371/journal.pone.0008773.g004

To confirm that the CCAAT-2 region is important in regulation of *MARCKS* transcription, we prepared several probes for the luciferase assay; D1-UTR(1152)-Luc which lacks the CCAAT-2 motif and its downstream region including Sp1 from UTR(1152)-Luc, D2-UTR(1152)-Luc which lacks the Sp1 region and downstream sequence from UTR(1152)-Luc, D3-UTR(1152)-Luc which lacks only sequence downstream of the Sp1 region, D4-UTR(1152)-Luc which lacks only the CCAAT-2 motif from

UTR(1152)-Luc, and M-UTR(1152)-Luc which has a point mutation in the CCAAT-2 motif (Figure 4B). Luciferase activity was detected from the SH-SY5Y cells transfected with each probe, and luciferase activity detected in the cells transfected with UTR(1152)-Luc was used as the baseline value (Figure 4B). Cells transfected with M-UTR(1152)-Luc and those transfected with D4-UTR(1152)-Luc exhibited marked increases in luciferase activity (Figure 4B), showing that the CCAAT-2 motif plays a key role in inhibition of *MARCKS* transcription. Furthermore, cells expressing D1-UTR(1152)-Luc, D2-UTR(1152)-Luc or D3-UTR(1152)-Luc exhibited no luciferase activity. These findings suggest that the sequence downstream of the Sp1 region, as well as the Sp1 region itself, is indispensable for *MARCKS* transcription.

To confirm the involvement of Dysbindin in the altered *MARCKS* transcription levels *via* the CCAAT-2 motif, we compared the luciferase activity of UTR(1152)-Luc detected in Dysbindin knockdown cells with that of control cells. As shown in Figure 4C, knockdown of Dysbindin resulted in upregulation of luciferase activity in the UTR(1152)-Luc transfected cells. However, the effect of knockdown of Dysbindin on luciferase activity was not observed in the D1-UTR(1152)-Luc transfected cells (Figure 4D). These results suggest that Dysbindin regulates *MARCKS* transcription *via* the CCAAT2 motif; the NF-YB binding site. On the other hand, since negligible levels of luciferase activity were observed in cells transfected with any of the probes lacking the sequence downstream of the Sp1 region, the sequence downstream of Sp1 appears to be essential for *MARCKS* transcription (Figure 4A and 4B).

Discussion

Numerous reports support the role of Dysbindin in the etiology of schizophrenia [13,30,37,53–60]. Previous studies have reported a decrease in Dysbindin expression in the brains of schizophrenic patients both at the mRNA and protein levels [26,27]. However, the functional involvement of Dysbindin in the neural system is not yet well elucidated. In this study, we examined involvement of Dysbindin in neural transmission and neural formation *via* transcriptional regulation, because abnormalities in these neural processes are very important in the pathogenesis of schizophrenia.

Regulation of *MARCKS* Transcription by the Dysbindin/NF-YB Interaction

As a result of the yeast-two-hybrid assay and immunoprecipitation assay, we revealed an interaction between NF-YB and Dysbindin (Figure 1 and 2). In addition, we showed the binding of NF-YB and Dysbindin to the *MARCKS* promoter region (Figure 3C). These findings suggest involvement of this complex in transcriptional regulation of MARCKS. As shown in Figure 4, we found two CCAAT sequence motifs at the 5′−UTR of the *MARCKS* gene. Previous reports show that members of the NF-Y family including NF-YB bind to CCAAT sequences and can regulate transcription of a number of genes. Our results suggest that one of the CCAAT sequences, CCAAT-2, is important for *MARCKS* transcriptional regulation. On the other hand, our luciferase assay results suggest that both the Sp1 region and the sequence downstream of Sp1 are indispensable for *MARCKS* transcription (Figure 4A and 4B).

Dysbindin Knockdown Increases MARCKS Protein Levels *In Vivo* and *In Vitro*

In accordance with the enhanced *MARCKS* transcription mediated by the knockdown of Dysbindin, Dysbindin knockdown cells show increased MARCKS levels (Figure 3A). Next, we examined the expression level of MARCKS in Dysbindin knockout mice. As shown in Figure 3b, in the wild-type mouse brain the peak in MARCKS expression is at postnatal day 15; thereafter decreasing markedly with advancing age until only low levels of MARCKS expression are seen in adults (P45). Comparable alternations in MARCKS expression were also observed in another mouse line, ICR (data not shown). These findings support the hypothesis that MARCKS plays an important role in brain development. However, in the Dysbindin knockout mice, there is no effect on MARCKS expression during the developmental stage, when MARCKS is abundantly expressed in wild-type mice. During this stage, *MARCKS* transcription may be regulated by multiple molecules, which compensate for the lack of Dysbindin. With increasing age of the mouse, MARCKS expression decreases gradually to a low level of expression in adults (Figure 3b). In contrast, a decrease in MARCKS expression was not observed in Dysbindin knockout mice (Figure 3b) and even in adult mice brains, a high level of expression of MARCKS was detected. These findings show that Dysbindin likely plays a major role in regulation of MARCKS expression in the adult brain, in contrast to in the developmental stage. Therefore, considering the results in Dysbindin knockout mice, it is likely that MARCKS is expressed at high levels in schizophrenic brains, compared with age-matched control brains.

MARCKS and Neural Transmission

It has been shown that MARCKS impacts on neurotransmission *via* F-actin and on vesicular transport *via* synaptic vesicles [46–48]. Furthermore, many reports indicate that dopaminergic transmission is increased in the brains of schizophrenics [1–4]. Dopamine D2 antagonists are an effective treatment in schizophrenia, and dopamine-enhancing drugs mimic psychotic symptoms of schizophrenia. In the schizophrenic brain, the expression of Dysbindin is decreased, resulting in an increase in MARCKS protein expression, which impacts on neurotransmission. Furthermore, we found that decreases in Dysbindin levels upregulate dopamine release [39]. Therefore, the enhanced dopaminergic transmission produced by the lower expression level of Dysbindin may be partially attributable to activation of MARCKS. Thus, the impairment of neural transmission in the schizophrenic brain may be caused by alterations of MARCKS expression levels *via* changes in Dysbindin.

Dysbindin May Regulate Neural Formation *via* Alteration of MARCKS Levels

Many studies support the hypothesis that schizophrenia is a neurodevelopmental disease. Disrupted-In Schizophrenia 1 (DISC1) is a gene disrupted by a (1;1) (q42.1; q14.3) translocation that segregates with major psychiatric disorders, including schizophrenia in a Scottish family [61,62]. Previously, we examined the physiological role of the molecular complex composed of DISC1 and its interacting partners, Fasciculation and elongation protein zeta 1 (Fez1) [63] and DISC1-Binding Zinc finger protein (DBZ)[64]. Both the DISC1-Fez1 interaction and the DISC1-DBZ interaction are involved in neurite extension. These reports suggest that abnormalities in the schizophrenia susceptibility genes, such as DISC1, likely cause an impairment of brain development resulting in schizophrenia. In addition, several reports suggest that the PKC signal is involved in psychiatric disorders, as well as other signals such as ERK, which play important roles in neural development. In addition, we previously showed the importance of Dysbindin for growth cone formation [40]. These previous reports suggest that abnormal neural formation could cause psychiatric disorders and that Dysbindin

may be one of the important factors in normal neural development. In this study, we demonstrate the transcriptional regulation of MARCKS *via* Dysbindin and the upregulation of MARCKS by downregulation of Dysbindin. Since MARCKS is involved not only in neural transmission[48] but also in neural developmental processes such as synaptogenesis and maintaining spine morphology [46,47], these results suggest that dysfunction of Dysbindin likely causes the upregulation of MARCKS and may induce abnormal development of the nervous system *via* alterations of MARCKS levels.

Thus, in this paper, we report the following findings; (1) Dysbindin interacts with NF-YB, (2) NF-YB and Dysbindin bind to the promoter region of MARCKS, (3) one of the CCAAT sequences is likely essential for the transcriptional regulation of MARCKS and (4) the downregulation of Dysbindin upregulates the expression of MARCKS *in vitro* and *in vivo*. On the other hand, we previously showed that Dysbindin knockout mice exhibit schizophrenia-like behavior and abnormalities of the dopaminergic system. These phenotypes may be at least partly attributable to over-activation of MARCKS *via* a decrease in Dysbindin levels.

In conclusion, these results may help shed some light on the causes of schizophrenia, and indicate that the transcriptional regulation of Dysbindin may contribute to schizophrenia. Further studies of Dysbindin and its association with MARCKS and with schizophrenia may reveal novel treatment targets for schizophrenia.

Materials and Methods

Antibodies

Monoclonal anti-Dysbindin antibody was produced. Briefly, GST-fused human Dysbindin was used as antigen and the Dysbindin protein for ELISA was made by thrombin digestion of GST-Dysbindin. High-titer clones for Dysbindin were selected by ELISA using the Dysbindin protein and the immunoreactivity of the clones was checked by Western blot. Antibodies of anti-GFP (Santa Cruz Biotechnology, Santa Cruz, CA), anti-Flag (Sigma-Aldrich, St Louis, MO), anti-V5 (Invitrogen), anti-β-actin (Chemicon International, Temecula, CA), anti-NF-YB (Santa Cruz Biotechnology), anti-MARCKS (Upstate), HRP-conjugated anti-mouse and Rabbit IgG (Cell Signaling Technology, Beverly, MA), and mouse normal IgG (Sigma-Aldrich) were purchased commercially.

Plasmids

We previously constructed the pEGFP-C1 expression vector (Clontech) carrying the full-length human *Dysbindin* cDNA (-GFP is tagged to N-terminal) [22]. The human Dysbindin-V5 (-V5 is tagged to C-terminal), Dysbindin-FLAG (-FLAG is tagged to N-terminal) and NF-YB moieties were amplified from a human brain cDNA library using PCR and subcloned into pcDNA3.1 (+) expression vector (Invitrogen, Carlsbad, CA). Dysbindin and NF-YB were amplified using rTaq DNA polymerase (Takara Bio Inc., Kyoto, Japan) with the following primer set: Dysbindin-V5, 5′−CTCGAGTTACGTAGAATCGAGACCGAGGAGAGGG-TTAGGGATAGGCTTACCAGAGTCGCTGTCCTCACC−3′-(forward) and 5′−GGTACCGCCACCATGCTGGAGACCCT-TCGCGA−3′ (reverse); NF-YB, 5′−GCTAGCGCCACCAT-GACAATGGATGGTGACAGTTCT−3′ (forward) and 5′−G-ATATCTGAAAACTGAATTTGCTGAAC−3′ (reverse). The amplified fragments were TA cloned into the pGEM-T vector (Promega Corp.).

pMARCKS-Luc(−1152) was generated by subcloning promoters into pGL3-(R2.2) Basic (Promega). We generated 5′ deletion constructs of pMARCKS-Luc(−1152) and an internal deletion construct of the region −700~−1. Other deletion constructs of the region (−231~−150) and point mutation constructs of pMARCKS-Luc/dl(−204~−187), were generated by inserting double-stranded oligonucleotides (Figure 2B and 2D). The plasmid pMARCKS-Luc(−736/mt) was generated by site-directed mutagenesis, which changed the same nucleotides as those of mutant 5.

Cell Culture

Human neuroblastoma SH-SY5Y cells were obtained from the Human Science Research Resources Bank (HSRRB). These cells were maintained in tissue culture dishes (Nalge Nunc, Rochester, NY, USA) in 50% minimal essential medium (Invitrogen) /50% F-12 (Invitrogen) containing 15% heat-inactivated fetal bovine serum (Invitrogen) at 37°C in an atmosphere of 95% air /5% CO_2.

Animals

sdy mice (Dysbindin KO mice) and wild-type littermates were provided by the Takeda lab, Department of Psychiatry, Osaka University Graduate School of Medicine. The mice were deeply anesthetized with sodium pentobarbital. Brains (hippocampus) were dissected from each aged mouse. All animal experiments were carried out in accordance with a protocol approved by the Institutional Animal Care and Use Committee of Osaka University.

Immunocytochemistry

SY5Y cells were grown on poly-l-lysine-coated four-well chamber dishes at a density of 3×10^4 cells/cm^2. The cells were fixed in 2% paraformaldehyde in 0.1 M PBS, permeabilized, and blocked with 0.02 M PBS containing 0.3% Triton X-100, 3% BSA and 10% goat serum for 30 min at room temperature, and then incubated with antibodies specific for the individual protein. Confocal microscopy was performed using a Carl Zeiss LSM-510 confocal microscope.

Fractionation Assay

Cells were collected after washing with ice-cold PBS. Cells and brains were homogenized in Tris buffer (20 mM Tris HCl, pH 7.8, 1 mM EDTA, 150 mM NaCl and protease inhibitor cocktail (Roche)). After homogenization, the homogenized proteins were lysed by the addition of 0.5% NP-40 for 30 min on ice and centrifuged at 500 ×*g* for 10 min to collect the nuclear pellet. The supernatant was collected as the cytosolic fraction.

Immunoprecipitation (IP)

After washing cells with ice-cold PBS, cells were collected and resuspended in 1 mL lysis buffer (20 mM Tris–HCl, pH 7.8, 0.2% NP-40, 1 mM EDTA, 150 mM NaCl and protease inhibitor cocktail (Roche)). Cells were frozen in dry ice/EtOH and stored at −80°C. Cell lysates were incubated on ice for 30 min and then centrifuged for 5 min at 13,600×*g*. After centrifugation, the supernatants were precleared with protein Sepharose G beads and IP was carried out in lysis buffer with antibody/protein G Sepharose beads for 1 h at 4°C. After washing in lysis buffer, immunoprecipitated proteins were immunoblotted.

Immunoblotting

Aliquots of whole cell lysates or IP lysates separated by SDS-PAGE were blotted onto an Immobilon-P membrane (Millipore), and then incubated with antibodies specific for individual protein. Proteins were detected by ECL plus Western Blotting Detection

System (GE Healthcare), followed by exposure to X-ray films according to the manufacturer's protocol.

Knockdown Experiment Using Small Interfering RNA (siRNA)

Stealth siRNA against Dysbindin (5′−CCAAAGUACUCUGCUGGAUUAGAAU−3′ and 5′−GCUCCCAGCUUUAAUCGCAGACUUA−3′), NF-YB 5′−UACUGAGGACAGCAUGAAUGAUCAU−3′ , and negative control duplexes (scrambled siRNA for Dysbindin, 5′−CCATGATCTCGTCGTTAGAAAGAAA−3′ and 5′−GCTACCGTTATTAGCACAGCCCTTA−3′ ; and scrambled siRNA for NF-YB, 5′−UACGGAACAACGAGUGUAUAUGCAU−3′) were provided by Invitrogen Corp. SY5Y cells were transfected with 100 pM of each siRNA and scrambled siRNA using Lipofectamine 2000 (Invitrogen Corp.) according to the manufacturer's instructions.

RNA Extracts and Microarray

Total RNA was extracted from cells using RNeasy columns (Qiagen) according to the manufacturer's instructions. Five hundred nanograms of total RNA from control and experimental cells was separately amplified and labeled with either Cy3- or Cy5-labeled CTP (Perkin Elmer) with an Agilent low input linear amplification kit (Agilent Technologies) according to manufacturer's instructions. After labeling and cleanup, amplified RNA was quantified by UV-vis spectroscopy. One microgram each of Cy3- and Cy5-labeled targets were combined and hybridized with a Whole Human Genome Oligo Microarray Kit (G4112F)according to the manufacturer's instructions. Three biological replicates were used at each time point with one of the replicates being a dye reversal of the other two. Microarrays were imaged on a Hitachi image scanner and data analyzed with GeneSpring 6 (Silicon Genetics).

Chromatin Immunoprecipitation (ChIP) Assay

ChIP analysis was performed using a Chromatin Immunoprecipitation Assay Kit (Upstate Biotechnology) according to the manufacturer's instructions. Briefly, protein−DNA complexes were crosslinked with 1% formaldehyde (10 min at room temperature) and cells were harvested. DNA was sonicated to lengths of 500−1000 bp. Antibodies specific for individual protein were used for immunoprecipitating protein-DNA complexes overnight at 4°C. PCR was performed with individual specific primer sets for the MARCKS promoter: the proximal CCAAT region, 5′−GGTTTGCTCTTTGATGCTCTTGAT−3′ and 5′−ACTTTCGGGTGGGGTGTAA−3′

Reporter Assay

Reporter plasmids were transfected into cells using Lipofectamine 2000 (Invitrogen) together with phRG-TK (Renilla reporter for internal control) which monitored transfection efficiency. Luciferase activities were assayed using the Dual Luciferase Assay System (Promega). All assays were performed three times in duplicate and values are shown as means ± SD.

Supporting Information

Figure S1 The preparation of mRNAs for microarray analysis. (A-(a) and B-(a)) To prepare RNAs for microarrays analysis, we transfected the siRNA for Dysbindin, NF-YB, or scrambled as a control. The effect of each RNAi was confirmed by Western blot using the antibody for Dysbindin or NF-YB. (A-(b) and B-(b)) The columns and vertical bars denote the means ± SEM (triplicate independent experiments; $P<0.001$, Student's t-test). Dysbindin or NF-YB was knocked-down significantly by transfection of the siRNA for Dysbindin or NF-YB, compared with the control.
Found at: doi:10.1371/journal.pone.0008773.s001 (1.10 MB EPS)

Acknowledgments

We thank Ms. Arakawa, Ms. Moriya, and Ms. Ohashi for preparing our experiments.

Author Contributions

Conceived and designed the experiments: HO SM SM MT. Performed the experiments: HO RK SM. Analyzed the data: HO RK SM SM NK TH RH TK MT. Contributed reagents/materials/analysis tools: SM NK SS KY KK RH MT TK. Wrote the paper: HO RK SM MT.

References

1. Garver DL (2006) Evolution of antipsychotic intervention in the schizophrenic psychosis. Curr Drug Targets 7(9): 1205-1215.
2. Lewis DA, Gonzalez-Burgos G (2006) Pathophysiologically based treatment interventions in schizophrenia. Nat Med 12(9): 1016-1022.
3. Ross CA, Margolis RL, Reading SA, Pletnikov M, Coyle JT (2006) Neurobiology of schizophrenia. Neuron 52(1): 139-153.
4. Mouri A, Noda Y, Enomoto T, Nabeshima T (2007) Phencyclidine animal models of schizophrenia: approaches from abnormality of glutamatergic neurotransmission and neurodevelopment. Neurochem Int 51(2-4): 173-184.
5. CATIE (Clinical Antipsychotic Trials of Intervention Effectiveness) investigators (2005) Effectiveness of antipsychotic drugs in patients with chronic schizophrenia. N Engl J Med 353: 1209-1223.
6. Coyle JT (2006) Glutamate and schizophrenia: Beyond the dopamine hypothesis. Cell Mol Neurobiol 26(4-6): 365-384.
7. Lau CG, Zukin RS (2007) NMDA receptor trafficking in synaptic plasticity and neuropsychiatric disorders. Nat Rev Neurosci 8(6): 413-26.
8. Li B, Woo RS, Mei L, Malinow R (2007) The neuregulin-1 receptor erbB4 controls glutamatergic synapse maturation and plasticity. Neuron 54(4): 583-97.
9. Moghaddam B (2003) Bringing order to the glutamate chaos in schizophrenia. Neuron 40: 881-884.
10. Snyder SH (2006) Dopamine receptor excess and mouse madness. Neuron 49: 484-485.
11. Stephan KE, Baldeweg T, Friston KJ (2006) Synaptic plasticity and dysconnection in schizophrenia. Biol Psychiatry 59(10): 929-39.
12. Straub RE, Jiang Y, MacLean CJ, Ma Y, Webb BT, et al. (2002) Genetic variation in the 6p22.3 gene DTNBP1, the human ortholog of the mouse dysbindin gene, is associated with schizophrenia. Am J Hum Genet 71: 337-348.
13. Schwab SG, Knapp M, Mondabon S, Hallmayer J, Borrmann-Hassenbach M, et al. (2003) Support for association of schizophrenia with genetic variation in the 6p22.3 gene, dysbindin, in sib-pair families with linkage and in an additional sample of triad families. Am J Hum Genet 72: 185-190.
14. Stefansson H, Sigurdsson E, Steinthorsdottir V, Bjornsdottir S, Sigmundsson T, et al. (2002) Neuregulin 1 and susceptibility to schizophrenia. Am J Hum Genet 71: 877-892.
15. Stefansson H, Sarginson J, Kong A, Yates P, Steinthorsdottir V, et al. (2003) Association of neuregulin 1 with schizophrenia confirmed in a Scottish population. Am J Hum Genet 72: 83-87.
16. Egan MF, Goldberg TE, Kolachana BS, Callicott JH, Mazzanti CM, et al. (2001) Effect of COMT Val108/158 Met genotype on frontal lobe function and risk for schizophrenia. Proc Natl Acad Sci U S A 98: 6917-6922.
17. Bilder RM, Volavka J, Czobor P, Malhotra AK, Kennedy JL, et al. (2002) Neurocognitive correlates of the COMT Val(158)Met polymorphism in chronic schizophrenia. Biol Psychiatry 52: 701-707.
18. Shifman S, Bronstein M, Sternfeld M, Pisante-Shalom A, Lev-Lehman E, et al. (2002) A highly significant association between a COMT haplotype and schizophrenia. Am J Hum Genet 71: 1296-1302.
19. Chowdari KV, Mirnics K, Semwal P, Wood J, Lawrence E, et al. (2002) Association and linkage analyses of RGS4 polymorphisms in schizophrenia. Hum Mol Genet 11: 1373-1380.
20. Williams NM, Preece A, Spurlock G, Norton N, Williams HJ, et al. (2004) Support for RGS4 as a susceptibility gene for schizophrenia. Biol Psychiatry 55: 192-195.
21. Chen X, Dunham C, Kendler S, Wang X, O'Neill FA, et al. (2004) Regulator of G-protein signaling 4 (RGS4) gene is associated with schizophrenia in Irish high density families. Am J Med Genet B Neuropsychiatr Genet 129: 23-26.
22. Morris DW, Rodgers A, McGhee KA, Schwaiger S, Scully P, et al. (2004) Confirming RGS4 as a susceptibility gene for schizophrenia. Am J Med Genet B Neuropsychiatr Genet 125: 50-53.

23. Wang S, Sun CE, Walczak CA, Ziegle JS, Kipps BR, et al. (1995) Evidence for a susceptibility locus for schizophrenia on chromosome 6pter-p22. Nat Genet 10: 41–46.
24. Straub RE, MacLean CJ, O'Neill FA, Burke J, Murphy B, et al. (1995) A potential vulnerability locus for schizophrenia on chromosome 6p24-22: evidence for genetic heterogeneity. Nat Genet 11: 287–293.
25. Benson MA, Newey SE, Martin-Rendon E, Hawkes R, Blake DJ (2001) Dysbindin, a novel coiled-coil-containing protein that interacts with the dystrobrevins in muscle and brain. J Biol Chem 276: 24232–24241.
26. Talbot K, Eidem WL, Tinsley CL, Benson MA, Thompson EW, et al. (2004) Dysbindin-1 is reduced in intrinsic, glutamatergic terminals of the hippocampal formation in schizophrenia. J Clin Invest 113(9): 1353–1363.
27. Weickert CS, Straub RE, McClintock BW, Matsumoto M, Hashimoto R, et al. (2004) Human dysbindin (DTNBP1) gene expression in normal brain and in schizophrenic prefrontal cortex and midbrain. Arch Gen Psychiatry 61(6): 544–55.
28. Chiba S, Hashimoto R, Hattori S, Yohda M, Lipska B, et al. (2006) Effect of antipsychotic drugs on DISC1 and dysbindin expression in mouse frontal cortex and hippocampus. J Neural Transm 113(9): 1337–46.
29. Bray NJ, Preece A, Williams NM, Moskvina V, Buckland PR, et al. (2005) Haplotypes at the dystrobrevin binding protein 1 (DTNBP1) gene locus mediate risk for schizophrenia through reduced DTNBP1 expression. Hum Mol Genet 14: 1947–1954.
30. Corvin A, Donohoe G, Nangle JM, Schwaiger S, Morris D, et al. (2008) A dysbindin risk haplotype associated with less severe manic-type symptoms in psychosis. Neurosci Lett 431(2): 146–149.
31. Donohoe G, Morris DW, Clarke S, McGhee KA, Schwaiger S, et al. (2007) Variance in neurocognitive performance is associated with dysbindin-1 in schizophrenia: a preliminary study. Neuropsychologia 45(2): 454–458.
32. Burdick KE, Lencz T, Funke B, Finn CT, Szeszko PR, et al. (2006) Genetic variation in DTNBP1 influences general cognitive ability. Hum Mol Genet 15(10): 1563–8.
33. Luciano M, Miyajima F, Lind PA, Bates TC, Horan M, et al. (2008) Variation in the dysbindin gene and normal cognitive function in three independent population samples. Genes Brain Behav.
34. Zinkstok JR, de Wilde O, van Amelsvoort TA, Tanck MW, Baas F, et al. (2007) Association between the DTNBP1 gene and intelligence: a case-control study in young patients with schizophrenia and related disorders and unaffected siblings. Behav Brain Funct 3: 19.
35. Sillitoe RV, Benson MA, Blake DJ, Hawkes R (2003) Abnormal dysbindin expression in cerebellar mossy fiber synapses in the mdx mouse model of Duchenne muscular dystrophy. J Neurosci 23(16): 6576–85.
36. Numakawa T, Yagasaki Y, Ishimoto T, Okada T, Suzuki T, et al. (2004) Evidence of novel neuronal functions of dysbindin, a susceptibility gene for schizophrenia. Hum Mol Genet 13: 2699–2708.
37. Murotani T, Ishizuka T, Hattori S, Hashimoto R, Matsuzaki S, et al. (2007) High dopamine turnover in the brains of Sandy mice. Neurosci Lett 421(1): 47–51.
38. Hattori S, Murotani T, Matsuzaki S, Ishizuka T, Kumamoto N, et al. (2008) Behavioral abnormalities and dopamine reductions in sdy mutant mice with a deletion in Dtnbp1, a susceptibility gene for schizophrenia. Biochem Biophys Res Commun 373(2): 298–302.
39. Kumamoto N, Matsuzaki S, Inoue K, Hattori T, Shimizu S, et al. (2006) Hyperactivation of Midbrain Dopaminergic System in Schizophrenia could be attributed to the Down-regulation of Dysbindin. Biochem Biophys Res Commun 345(2): 904–905.
40. Kubota K, Kumamoto N, Matsuzaki S, Hashimoto R, Hattori T, et al. (2009) Dysbindin engages in c-Jun N-terminal kinase activity and cytoskeletal organization. Biochem Biophys Res Commun 379: 191–195.
41. Donati G, Imbriano C, Mantovani R (2006) Dynamic recruitment of transcription factors and epigenetic changes on the ER stress response gene promoters. Nucleic Acids Res 34(10): 3116–27.
42. Gurtner A, Manni I, Fuschi P, Mantovani R, Guadagni F, et al. (2003) Requirement for down-regulation of the CCAAT-binding activity of the NF-Y transcription factor during skeletal muscle differentiation. Mol Biol Cell 14(7): 2706–15.
43. Li Q, Herrler M, Landsberger N, Kaludov N, Ogryzko VV, et al. (1998) Xenopus NF-Y pre-sets chromatin to potentiate p300 and acetylation-responsive transcription from the Xenopus hsp70 promoter in vivo. EMBO J 17(21): 6300–15.
44. Maity SN, de Crombrugghe B (1998) Role of the CCAAT-binding protein CBF/NF-Y in transcription. Trends Biochem Sci 23(5): 174–8.
45. Nian H, Fan C, Liao S, Shi Y, Zhang K, et al. (2007) RNF151, a testis-specific RING finger protein, interacts with dysbindin. Arch Biochem Biophys 465(1): 157–163.
46. Trifaró J, Rosé SD, Lejen T, Elzagallaai A (2000) Two pathways control chromaffin cell cortical F-actin dynamics during exocytosis. Biochimie 82(4): 339–352.
47. Sasaki Y (2003) New aspects of neurotransmitter release and exocytosis: Rho-kinase-dependent myristoylated alanine-rich C-kinase substrate phosphorylation and regulation of neurofilament structure in neuronal cells. J Pharmacol Sci 93(1): 35–40.
48. Park YS, Hur EM, Choi BH, Kwak E, Jun DJ, et al. (2006) Involvement of protein kinase C-epsilon in activity-dependent potentiation of large dense-core vesicle exocytosis in chromaffin cells. J Neurosci 26(35): 8999–9005.
49. Maejima T, Oka S, Hashimotodani Y, Ohno-Shosaku T, Aiba A, et al. (2005) Synaptically driven endocannabinoid release requires Ca2+-assisted metabotropic glutamate receptor subtype 1 to phospholipase Cbeta4 signaling cascade in the cerebellum. J Neurosci 25(29): 6826–35.
50. Koh TW, Bellen HJ (2003) Synaptotagmin I, a Ca2+ sensor for neurotransmitter release. Trends Neurosci 26(8): 413–22.
51. Manji HK, Lenox RH (1999) Protein kinase C signaling in the brain: molecular transduction of mood stabilization in the treatment of manic-depressive illness. Biol Psychiatry 46(10): 1328–51.
52. Sokolov BP, Tcherepanov AA, Haroutunian V, Davis KL (2000) Levels of mRNAs encoding synaptic vesicle and synaptic plasma membrane proteins in the temporal cortex of elderly schizophrenic patients. Biol Psychiatry 48(3): 184–96.
53. van den Bogaert A, Schumacher J, Schulze TG, Otte AC, Ohlraun S, et al. (2003) The DTNBP1 (dysbindin) gene contributes to schizophrenia, depending on family history of the disease. Am J Hum Genet 73: 1438–1443.
54. Tang JX, Zhou J, Fan JB, Li XW, Shi YY, et al. (2003) Family-based association study of DTNBP1 in 6p22.3 and schizophrenia. Mol Psychiatry 8: 717–718.
55. van den Oord EJ, Sullivan PF, Jiang Y, Walsh D, O'Neill FA, et al. (2003) Identification of a high-risk haplotype for the dystrobrevin binding protein 1(DTNBP1) gene in the Irish study of high-density schizophrenia families. Mol Psychiatry 8: 499–510.
56. Williams NM, Preece A, Morris DW, Spurlock G, Bray NJ, et al. (2004) Identification in 2 independent samples of a novel schizophrenia risk haplotype of the dystrobrevin binding protein gene (DTNBP1). Arch Gen Psychiat 61: 336–344.
57. Funke B, Finn CT, Plocik AM, Lake S, DeRosse P, et al. (2004) Association of the DTNBP1 locus with schizophrenia in a U.S. population. Am J Hum Genet 75: 891–898.
58. Kirov G, Ivanov D, Williams NM, Preece A, Nikolov I, et al. (2004) Strong evidence for association between the dystrobrevin binding protein 1 gene (DTNBP1) and schizophrenia in 488 parent-offspring trios from Bulgaria. Biol Psychiatry 55: 971–975.
59. Fanous AH, van den Oord EJ, Riley BP, Aggen SH, Neale MC, et al. (2005) Relationship between a high-risk haplotype in the DTNBP1 (dysbindin) gene and clinical features of schizophrenia. Am J Psychiatry 162: 1824–1832.
60. Gornick MC, Addington AM, Sporn A, Gogtay N, Greenstein D, et al. (2005) Dysbindin (DTNBP1, 6p22.3) is Associated with Childhood-Onset Psychosis and Endophenotypes Measured by the Premorbid Adjustment Scale (PAS). J Autism Dev Disord 10: 1–8.
61. Millar JK, Wilson-Annan JC, Anderson S, Christie S, Taylor MS, et al. (2000) Disruption of two novel genes by a translocation co-segregating with schizophrenia. Hum Mol Genet 9: 1415–1423.
62. Millar JK, Christie S, Anderson S, Lawson D, Hsiao-Wei LD, et al. (2001) Genomic structure and localisation within a linkage hotspot of Disrupted In Schizophrenia 1, a gene disrupted by a translocation segregating with schizophrenia. Mol Psychiatry 6: 173–178.
63. Miyoshi K, Honda A, Baba K, Taniguchi M, Oono K, et al. (2003) *Disrupted-In-Schizophrenia 1*, a candidate gene for schizophrenia, participates in neurite outgrowth. Mol Psychiatry 8: 685–694.
64. Hattori T, Baba K, Matsuzaki S, Honda A, Miyoshi K, et al. (2007) A novel DISC1-interacting partner DISC1-Binding Zincfinger protein: implication in the modulation of DISC1-dependent neurite outgrowth. Mol Psychiatry 12: 398–407.

OPEN ACCESS Freely available online

PLoS one

Increased Stathmin1 Expression in the Dentate Gyrus of Mice Causes Abnormal Axonal Arborizations

Kohei Yamada[1☯], Shinsuke Matsuzaki[2☯], Tsuyoshi Hattori[3], Ryusuke Kuwahara[1], Manabu Taniguchi[1], Hitoshi Hashimoto[2,4], Norihito Shintani[3,4], Akemichi Baba[4], Natsuko Kumamoto[1], Kazuo Yamada[5], Takeo Yoshikawa[5], Taiichi Katayama[2]*, Masaya Tohyama[1,2]

1 Department of Anatomy and Neuroscience, Graduate School of Medicine, Osaka University, Suita, Osaka, Japan, **2** United Graduate School of Child Development, Osaka University, Kanazawa University and Hamamatsu University School of Medicine, Suita, Osaka, Japan, **3** Department of Molecular Neuropsychiatry, Graduate School of Medicine, Osaka University, Suita, Osaka, Japan, **4** Laboratory of Molecular Neuropharmacology, Graduate School of Pharmaceutical Sciences, Osaka University, Suita, Osaka, Japan, **5** Laboratory of Molecular Psychiatry, RIKEN Brain Science Institute, Wako, Saitama, Japan

Abstract

Pituitary adenylate cyclase-activating polypeptide (PACAP) is involved in multiple brain functions. To clarify the cause of abnormal behavior in PACAP deficient-mice, we attempted the identification of genes whose expression was altered in the dentate gyrus of PACAP-deficient mice using the differential display method. Expression of stathmin1 was up-regulated in the dentate gyrus at both the mRNA and protein levels. PACAP stimulation inhibited stathmin1 expression in PC12 cells, while increased stathmin1expression in neurons of the subgranular zone and in primary cultured hippocampal neurons induced abnormal arborization of axons. We also investigated the pathways involved in PACAP deficiency. Ascl1 binds to E10 box of the stathmin1 promoter and increases stathmin1 expression. Inhibitory bHLH proteins (Hes1 and Id3) were rapidly up-regulated by PACAP stimulation, and Hes1 could suppress Ascl1 expression and Id3 could inhibit Ascl1 signaling. We also detected an increase of stathmin1 expression in the brains of schizophrenic patients. These results suggest that up-regulation of stathmin1 in the dentate gyrus, secondary to PACAP deficiency, may create abnormal neuronal circuits that cause abnormal behavior.

Citation: Yamada K, Matsuzaki S, Hattori T, Kuwahara R, Taniguchi M, et al. (2010) Increased Stathmin1 Expression in the Dentate Gyrus of Mice Causes Abnormal Axonal Arborizations. PLoS ONE 5(1): e8596. doi:10.1371/journal.pone.0008596

Editor: Tadafumi Kato, RIKEN Brain Science Institution, Japan

Received August 25, 2009; **Accepted** December 2, 2009; **Published** January 6, 2010

Funding: This work was supported in part by Osaka University operating budget. The funders had no role in study design, data collection and analysis, decision to publish, or preparation of the manuscript.

Competing Interests: The authors have declared that no competing interests exist.

* E-mail: katayama@ugscd.osaka-u.ac.jp

☯ These authors equally contributed to this work.

Introduction

PACAP is a neuropeptide that is expressed in the brain as well as in the neurons of a number of peripheral organs and it is involved in various neurobiological functions, such as neurotransmission and neural plasticity [1,2]. It also has a neurotrophic effect via three heptahelical G protein-coupled receptors, one of which is specific for PACAP (PAC_1 receptor) and two others that are shared with vasoactive intestinal polypeptide ($VPAC_1$ and $VPAC_2$ receptors) [3]. Recently, mice that lack *Adcyap1*, the gene encoding PACAP, (*Adcyap1*$^{-/-}$ mice) were developed [2,4]. *Adcyap1*$^{-/-}$ mice display remarkable behavioral abnormalities providing evidence that PACAP plays a previously uncharacterized role in the regulation of psychomotor behavior. When placed into a novel environment, such as an open field, the mutants display significantly increased locomotor activity with minimal time spent habituating themselves to the environment, and less time engaged in licking and grooming behavior. The mutants also show explosive jumping behavior in the open field and increased exploratory behavior [2,5]. These behavioral abnormalities may be due to perturbation of monoamine neurotransmission because serotonin metabolite 5-hydroxyindoleacetic acid is slightly decreased in the cerebral cortex and striatum of PACAP-deficient mice, and hyperactive behavior is ameliorated by the antipsychotic drug, haloperidol [2]. In addition, the jumping behavior is suppressed by drugs that elevate extracellular serotonin, such as the selective serotonin reuptake inhibitors [6]. *Adcyap1*$^{-/-}$ mice also showed increased immobility in a forced swimming test, which was reduced by the antidepressant, desipramine [7]. In addition it is known that PAC_1-deficient mice exhibit reduced social behavior [8]. And, it is also known that PAC_1-deficient mice exhibit increased fear conditioning and a reduction of LTP [9]. A previous association study reported that several single nucleotide polymorphisms (SNPs) in the vicinity of the PACAP gene locus were associated with schizophrenia [10]. However, none of genome wide association studies showed association of this gene with schizophrenia [11]. *Disrupted-In-Schizophrenia 1* (*DISC1*) has been identified as a potential susceptibility gene for major psychiatric disorders [12,13]. We previously identified several DISC1-interacting factors [14,15,16]. DISC1-binding zinc finger protein (DBZ) is one of these factors. We found that PACAP up-regulates DISC1 expression and markedly reduced the association of DISC1 with DBZ in PC12 cells, and that a DISC1-binding domain of DBZ reduces neurite length in PC12 cells following

PACAP stimulation in primary cultured hippocampal neurons [12]. Therefore, these results suggest that PACAP may play a role in mental disorders such as schizophrenia.

However, nothing is known about the mechanisms of PACAP deficiency-induced psychiatric illness, so this study was performed to investigate these mechanisms.

The localization of PAC_1 mRNA in the neurons of rat and mice brains has been examined by *in situ* hybridization [17]. Neurons showing intense signals for PAC_1 mRNA were found in the dentate gyrus of the hippocampus, olfactory bulb, second layer of the cerebral cortex, and several hypothalamic areas. In addition, an atrophy of the hippocampus had been reported in schizophrenic patients [10]. To elucidate molecular events associated with PACAP deficiency in the mouse brain that could be relevant to schizophrenia, therefore we attempted to detect PACAP deficiency-regulated genes in the dentate gyrus using the differential display (DD) method and found that stathmin1 expression was up-regulated in the dentate gyrus of PACAP-deficient mice. Stathmin1 is expressed at high levels by neurons and glial cells of the brain [18,19]. It interacts with tubulin and destabilizes microtubules [20]. However, the detailed functions and regulatory mechanisms of stathmin1 in the formation of neural networks are unclear.

In this study, we found that an increase of stathmin1 expression induced abnormal sprouting of neurons in the dentate gyrus, and we showed that stathmin1 was regulated by a basic helix loop helix (bHLH) factor via a PACAP-dependent molecular signaling pathway.

Methods

Animals

Adcyap$^{-/-}$ mice and wild-type littermates were provided by the Baba lab, Laboratory of Molecular Neuropharmacology, Graduate School of Pharmaceutical Sciences, Osaka University. Pregnant female rats were deeply anesthetized with sodium pentobarbital. Brains were dissected from day 18 embryos and cultured. All animal experiments were carried out in accordance with a protocol approved by the Institutional Animal Care and Use Committee of Osaka University.

Construction of the stathmin1, Ascl1, Hes1 and Id3 expression vectors

Mouse stathmin1 cDNA was subcloned into pEGFP-C3 (Clontech) to generate stathmin1 with green fluorescent protein (GFP) fused to the N-terminal (GFP-stathmin1) and into a bicistronic expression vector (pIRES2-EGFP; Clontech) to produce stathmin1-IRES-GFP. A mouse Hes1 expression plasmid, pCI-Hes1, and Hes1 antibody were kind gifts from Prof. R. Kageyama. Rat Ascl1 and Id3 were sub-cloned into pCI-neo (Clontech).

Cell culture and transfection

PC12 cells were cultured in Dulbecco's modified Eagle's medium (DMEM) containing 10% horse serum and 5% FBS in a 5% CO_2/95% air humidified atmosphere at 37°C. Twenty four hours after plating, PACAP was applied. The inhibitors were added 1 h before PACAP treatment. Rat primary hippocampal neurons were prepared from day 18 embryos using nerve cell culture system MB-X9901 (Sumitomo Bakelite, Tokyo, Japan) as described in the Sumilon Protocol N-4.2. Neurons were plated on poly-L-lysine coated chamber slides and cultured in MEM with 5% FCS in a 5% CO_2/95% air humidified atmosphere at 37°C. Approximately 1×10^5 neurons or 6×10^5 PC12 cells were transfected with 2 μg or 1 μg of pGFP-Stathmin1, pStathmin1-IRES-GFP or a GFP only expression vector using Lipofectamine 2000 (Invitrogen, Carlsbad, CA, USA).

Construction of rat stathmin1 promoter-luciferase plasmids

Rat stathmin1 genomic sequence (PubMed accession no. NC_005104) was identified using a BLAST search with stathmin1 cDNA sequence, and a 1.9 kb region corresponding −1534 to +325 was amplified by PCR using forward primer 5′- and reverse primer 5′- containing KpnI and NheI sites and subcloned into the KpnI-NheI site of the pGL3 basic vector. This plasmid is designated as STMN1-1. Deletion constructs, STMN1-2 (−1343/+325), STMN1-3 (−1264/+325) and STMN1-4 (−1152/+325) were produced by fill-in reaction with DNA polymerase (Klenow fragment) and blunt end ligation.

Transient transfection and luciferase assays

Transient transfections with various promoter constructs were performed using Lipofectamine (Invitrogen, Carlsbad, CA, USA) according to the manufacturer's instructions. Cells in 6-well dishes were transfected with either 0.1 μg of empty pGL3vector or with promoter-reporter constructs (STMN1-1, STMN1-2, STMN1-3 and STMN1-4), along with 1 ng Renilla luciferase plasmid pRL. In co-transfection experiments, different amounts of Ascl1, Id3 and Hes1 expression plasmids were added. The total amount of DNA added in each transfection was kept constant by addition of an empty control vector. 48 h after transfection, cells were washed with pre-chilled PBS and lysed in passive lysis buffer (Dual Luciferase kit, Promega). Firefly luciferase and Renilla luciferase activities in the cell lysates were measured according to the manufacturer's instructions using a TD 20/20-luminometer (Turner Biosystems, Sunnyvale, CA, USA). Firefly luciferase activity was normalized to the Renilla luciferase activity and reported as relative luciferase activity (RLA).

Preparation of RNA and Real-Time RT-PCR

The hippocampus was rapidly dissected from each brain, and the hippocampus was divided into Ammon's horn and the dentate gyrus [21]. Preparations of total RNA from the tissues were performed as previously described [22]. Total RNA was isolated from PC12 cells using the RNA Easy Kit (Qiagen, Tokyo, Japan). Each RNA was transcribed to cDNA using reverse transcription reagents (Superscript III; Invitrogen or High-Capacity cDNA Reverse Transcription Kit; Applied Biosystems) according to the manufacturer's instructions.

Real-time RT-PCR was performed on a thermocycler (7900HT Sequence Detection Systems; Applied Biosystems, Foster, CA, USA) with nuclear stain reagents (SYBR Green; Applied Biosystems), according to the manufacturer's instructions. Amplification of PCR products was measured by fluorescence associated with the binding of double-stranded DNA to the SYBR green dye in the reaction mixture. Quantification of each PCR product was expressed relative to GAPDH. The following primers were used: mouse stathmin1; forward, 5′-ccaggcttttgagctgattc; reverse, 5′-gcgtctttcttctgcagctt, mouse GAPDH; forward, 5′-attgtggaagggctcatgacc; reverse, 5′-atgcagggatgatgttctggg, rat stathmin1; forward, 5′-aatggcagaggagaaactgacc; reverse, 5′-cgtgcttgtccttctctcgc, rat Id3; forward, 5′-acatgaaccactgctactcgcg; reverse, 5′-cagaaccacttgaaggtcgagg, rat Hes1; forward, 5′-aaatgacagtgaagcacctccg; reverse, 5′-ttaacgccctcacacgtgg, rat Ascl1; forward, 5′- ttaacctgggctttgccac; reverse, 5′- agcgcgcggatgtattc, rat GAPDH; forward, 5′- gccttctcttgtgacaaagtgg; reverse, 5′-attctcagccttgactgtgcc.

Chromatin immunoprecipitation (ChIP Assay)

ChIP assays were performed using a ChIP kit (Millipore TM) following the manufacturer's protocol. Briefly, PC12 cells were cross-linked, chromatin was prepared and immunoprecipitated with anti-Ascl1 antibody (Santa Cruz) or with control IgG. Then, immunoprecipitated DNA was eluted and PCR amplified using appropriate primers. For PCR amplification of the E10–11 box (40 cycles), the E10 box (50 cycles) and the negative control (N.C.) (55 cycles), the following primers were used: E10-E11-forward, 5′-tgcctctataagcatattttacgc; E10-E11-reverse, 5′-atttggtctcccaaaagc-taaacc; E10-forward, 5′-cagttttcattgtcttgtatgcctg; E10-reverse, 5′-atttggtctcccaaaagctaaacc; N.C.-forward, 5′-gctccgatctcattgttgg; N.C.-reverse, 5′-tcatctagaaacaccgaagcc.

Immunoblot analysis

Lysates of PC12 cells and of hippocampal dentate gyrus were used directly for western blot analysis as described previously [14,21]. The following antibodies were employed: rabbit polyclonal anti-stathmin1 (GeneTex). Goat anti-rabbit or anti-mouse IgG conjugated with horseradish peroxidase (Cell Signaling Technology, Beverly, MA, USA) were used as the secondary antibodies. Reaction products were visualized by detection of chemiluminescence using an ECL kit (Amersham Biosciences, Piscataway, NJ, USA). Quantitation of relative band densities was performed by scanning densitometry. All experiments were repeated independently at least three times. PC12 cells were cultured for 1 day at a low cell density, starved of serum for 4 h, and then treated with 100 nM PACAP (PACAP-38) (Peptide Institute, Mino, Osaka, Japan). Cells were harvested at the indicated times after PACAP stimulation.

Immunohistochemistry

Sections (20 μm) were prepared from frozen brains using a cryostat and thaw-mounted on APS coated slides (Matsunami, Japan) and stored in a tightly closed case at −80°C. The following antibodies were employed: rabbit polyclonal anti-stathmin1 (GeneTex), mouse monoclonal anti-MAP2 (Sigma), anti-Tau (Sigma), and anti-Ascl1 (Santa Cruz Biotechnology). Floating sections were incubated with these antibodies overnight at 4°C. Confocal microscopy was performed using an LSM-510 laser scanning microscope (Carl Zeiss, Oberkochen, Germany).

Quantification of stathmin1 positive cells in the subgranular zone (SGZ) and of dot fibers in the hilus

Stathmin1 cells were counted in coronal sections. The entire DG region of each hippocampus was imaged as a z-series of 20 μm-thick sections. All data analysis was blind to genotype. Statistical analysis was performed using Student's t-test.

After immunolabeling for stathmin1 in equivalent coronal sections, a 20 μm-thick z-series of confocal images was collected in dentate gyrus of hippocampus.

Double labeling with *in situ* hybridization and immunohistochemistry

The protocol for the *in situ* hybridization (ISH) histochemistry was modified from a previously published method [23]. cDNA fragments of rat PAC_1 were amplified by RT-PCR using the oligonucleotide primers 5′-cttgtacagaagctgcagtc-3′ (sense) and 5′-ggtgcttgaagtccatagtg-3′ (antisense) and then used as templates for probe synthesis. For double ISH and immunohistochemistry, sections were immunostained followed by ISH. The protocol for immunohistochemistry was based on the published ABC method (Elite ABC kit; Vector, CA, USA) using the rabbit anti-stathmin1 primary antibody at 1:500. The specificity of the immunohistochemistry was checked by omitting the primary antibody.

Immunoelectron microscopy

Eight week-old mice were deeply anesthetized with sodium pentobarbital and perfused transcardially with 0.85% physiological saline followed by 0.05% glutaraldehyde and 4% paraformaldehyde in a 0.1 M phosphate buffer (pH 7.4). Brains were removed and post-fixed in the same fixative for 4 h at 4°C, followed by immersion in 30% sucrose in 0.1 M PB overnight at 4°C. 20 μm brains sections were then cut on a cryostat. Immunohistochemistry was performed using free-floating sections according to the ABC method. The anti-stathmin antibodies were used at a dilution of 1:1000. Biotinylated anti-rabbit IgG (Vectastain Elite) was used as a secondary antibody. Immunoreactivity was visualized with 0.05% diaminobenzidine and 0.01% hydrogen peroxide in 50 mM Tris, pH 7.6. These sections were washed several times in a 0.1 M phosphate buffer (pH 7.4) and after post-fixation with 1% OSO_4 for 1 h and dehydration they were flat-embedded in Epon 812. Ultrathin sections were viewed without uranyl acetate or lead citrate staining using an H-7000 electron microscope (Hitachi).

Quantitative RT-PCR assays using Postmortem Brain samples

RNA samples from the dorsolateral prefrontal cortex (DLPFC; Brodmann's area 46) were obtained from the Stanley Medical Research Institute (http://www.stanleyresearch.org/programs/brain_collection.asp). Samples were taken from 35 schizophrenics (26 males, 9 females; mean±SD age, 42.6±8.5 years; postmortem interval (PMI), 31.4±15.5 h; brain pH, 6.5±0.2), 35 bipolar disorder patients (17 males, 18 females; mean±SD age, 45.3±10.5 years; PMI, 37.9±18.3 h; brain pH, 6.4±0.3), and 35 controls (26 males, 9 females; mean±SD age, 44.2±7.6 years; PMI, 29.4±12.9 h; brain pH, 6.6±0.3). Diagnoses were made by applying DSM-IV (the Diagnostic and Statistical Manual of Mental Disorders, Fourth Edition) criteria. All schizophrenic patients were medicated with anti-psychotics. Quantitative RT-PCR analysis was conducted using an ABI7900HT Fast Real-Time PCR System (Applied Biosystems) with TaqMan Gene Expression Assays (Applied Biosystems). All quantitative RT-PCR reactions were performed in triplicate, based on a standard curve method. Detection values are normalized according to the internal controls (GAPDH, ACTB and PGK1). TaqMan probes for STMN1, GAPDH, ACTB, and PGK1 were selected from predesigned TaqMan Gene Expression Assays (AssayID: STMN1, Hs01027516_g1; GAPDH, Hs99999905_m1; ACTB, Hs99999903_m1; PGK, Hs99999906_m1). The Mann-Whitney U test (two-tailed) was used to detect significant changes in target gene expression levels.

Association Study Subjects

The case-control samples consisted of 1060 unrelated schizophrenic patients (503 men, 557 women; mean age 48.0±13.8 years) and 1060 age- and sex-matched controls (503 men, 557 women; mean age 47.7±13.6 years). All patients had a consensual diagnosis of schizophrenia according to DSM-IV criteria from at least two experienced psychiatrists. Control subjects were recruited from hospital staff and volunteers who showed no present or past evidence of psychoses, during brief interviews by psychiatrists. All participants were recruited from a geographic area located in central Japan. The current study was approved by the Ethics Committees of RIKEN. All participants provided written informed consent.

SNPs and Genotyping

Three SNPs, rs159522, rs12037513 and rs807061 located in close vicinity of the STMN1 gene were genotyped in this study. SNP genotyping was performed using the TaqMan system (Applied Biosystems, Foster City, CA, USA) according to the recommendations of the manufacturer. PCR was performed using an ABI 9700 thermocycler. Fluorescent signals were analyzed using an ABI7900HT Fast Real-Time PCR System and SDS v2.3 software (Applied Biosystems).

Statistical Analyses

Concerning the association study, analysis of the significance of differences in mRNA expression between the control group and the chronic stress group was performed using Student's t-test. The allelic and genotypic distributions in the Japanese case-control samples were tested for association by Fisher's exact test. Haplotypic association analysis of Japanese samples was performed using the COCAPHASE program in the UNPHASED v3.0.11 program (http://www.mrc-bsu.cam.ac.uk/personal/frank/software/unphased/) [Dudbridge, 2008]. To estimate the degree of linkage disequilibrium (LD), the standardized disequilibrium coefficient (D') and the squared correlation coefficient (r2) were calculated using Haploview 4.0 (http://www.broad.mit.edu/mpg/haploview/). The deviation of genotype distributions from the Hardy–Weinberg equilibrium (HWE) was evaluated by the chi-squared test (d.f. = 1). Other results were expressed as the mean±SE, with statistical analysis being performed by a one way ANOVA.

Results

Down-regulation of PACAP expression induces up-regulation of stathmin1 expression in the dentate gyrus both *in vivo* and *in vitro*

To detect the genes regulated by PACAP, we searched for gene transcripts that were clearly up-regulated or down-regulated in the dentate gyrus of *Adcyap*$^{-/-}$ mice.

The differential display (DD) method showed that 55 cDNA fragments were up-regulated or down-regulated in the dentate gyrus of *Adcyap*$^{-/-}$ mice compared with wild-type mice. One of these genes, stathmin1, was subjected to further analysis. Real-time PCR showed that stathmin1 mRNA was markedly increased in the dentate gyrus of *Adcyap*$^{-/-}$ mice (Fig. 1A). Increased stathmin1 protein levels in the dentate gyrus of *Adcyap*$^{-/-}$ mice were also confirmed by western blot analysis (Fig. 1B). Thus, PACAP deficiency induced elevation of stathmin1 in the dentate gyrus.

We then examined whether the *in vivo* changes described above could be reproduced *in vitro* using PC12 cells. Stathmin1 mRNA levels were decreased 3 hours after PACAP stimulation, and expression continued to decrease over the next 24 hours (Fig. 1C). PACAP stimulation of PC12 cells caused stathmin1 protein levels to decrease (Fig. 1D), and also caused a dose-dependent decrease of stathmin1 mRNA levels (Fig. 2A). The decrease of stathmin1 expression by PACAP stimulation was slightly, but statistical significantly, inhibited by pretreatment with a PAC_1/$VPAC_2$ receptor antagonist (PACAP6-38) (Fig. 2B). We did not perform the Western blot analysis, because we assumed that this small difference would not be detectable due to the limitation of its sensitivity. Pretreatment with a p38 antagonist (SB202190) or an ERK antagonist (PD98059) also inhibited the decrease of stathmin1 expression by PACAP (Fig. 2C). Co-administration of SB202190 and PD98059 strongly inhibited the effect of PACAP (Fig. 2C). The p38 and ERK are key elements of the PACAP signaling pathway (supplementary Fig. S1). On the other hand, VIP did not decrease stathmin1 expression (Fig. 2D). These results indicate that PACAP inhibits stathmin1 expression in PC12 cells. Furthermore, we showed that PACAP regulates stathmin1 expression via the PAC_1 receptor in neurons of the dentate gyrus subgranular zone, as described below.

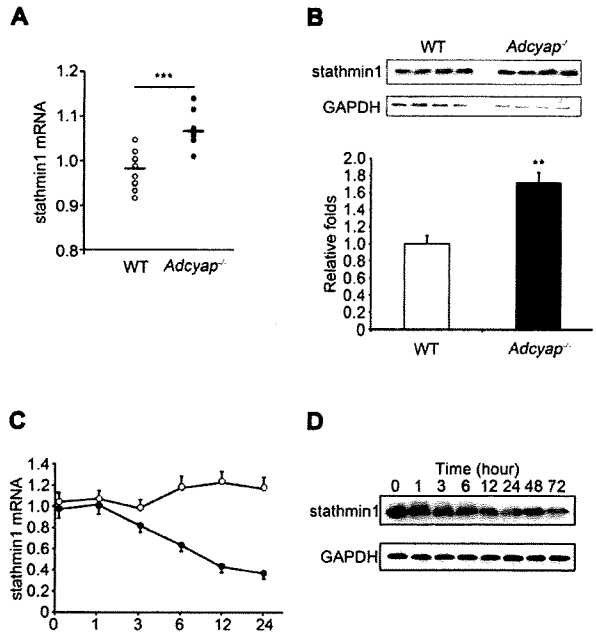

Figure 1. Stathmin1 expression is negatively controlled by PACAP. (A, B) Comparison of stathmin1 expression of wild-type mice to that of *Adcyap*$^{-/-}$ mice. (A) Expression level of stathmin1 mRNA in DG was measured by real-time RT-PCR and normalized to the expression of GAPDH. Data represents means±SEM of independent experiments (wild type n = 10, *Adcyap*$^{-/-}$ n = 10, ***P = 0.0000496 compared with wild type). (B) Expression of stathmin1 protein in the DG of wild type and *Adcyap*$^{-/-}$ mice measured by western blot analysis (upper panel). GAPDH was used as internal control (middle panel). Lower panel shows the ratio of stathmin1 protein level in DG of *Adcyap*$^{-/-}$ mice (closed column) to that of wild-type mice (open column). Error bars represent ±SEM. (wild-type n = 4, *Adcyap*$^{-/-}$ n = 4, **P = 0.00277 compared with wild-type). (C, D) Kinetic studies of the effect of PACAP signaling on stathmin1 expression levels in PC12 cells. (C) Alteration of stathmin1 mRNA levels by the indicated period of PACAP (100 nM) stimulation was quantified by real-time PCR. Data are expressed as mean percentages ±SEM relative to control values at 0 h. Open circle indicates vehicle treatment. Closed circle represents PACAP treatment. (D) Alteration of stathmin1 protein levels under the indicated period of PACAP (100 nM) stimulation was measured by western blot analysis using an anti-stathmin1 antibody.
doi:10.1371/journal.pone.0008596.g001

Up-regulation of stathmin1 induces abnormal axonal arborization in neurons of the dentate gyrus subgranular zone

Stathmin1 is mainly localized in subgranular zone neurons with prominent localization in cell processes. Immunohistochemistry for stathmin1 in the dentate gyrus of wild-type mice showed that cells expressing stathmin1 were preferentially localized in the innermost part of the granular cell layer, the so-called subgranular zone (SGZ) where neurogenesis of granular cells occurs in adults (Fig. 3A, B). A large number of cells in the SGZ expressed stathmin1. Immunohistochemical analysis also

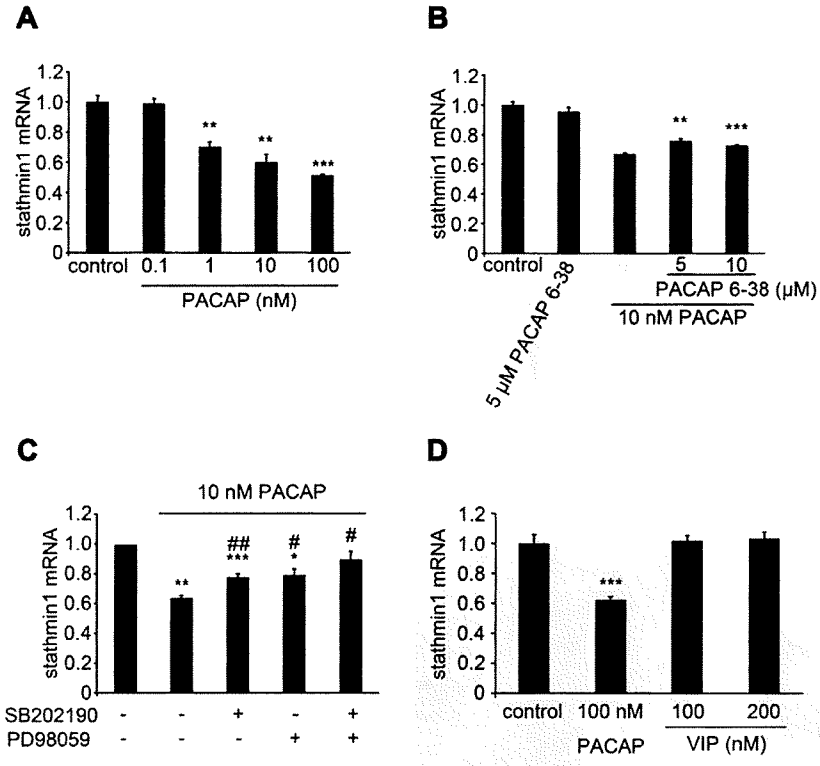

Figure 2. PACAP regulated stathmin1 expression via PAC_1 in PC12 cells. (A) Alteration of stathmin1 mRNA levels 24 hours after PACAP treatment, at indicated concentrations, was quantified by real-time PCR. Data are expressed as mean percentages ±SEM relative to control values (n = 3, PACAP 1 nM **P = 0.0044, 10 nM **P = 0.0033, 100 nM ***P = 0.0003 compared with control). (B, C) Effect of PACAP signaling pathway inhibitors on the PACAP-induced down-regulation of stathmin1 expression. (B) PC12 cells were treated with 10 nM PACAP for 6 h and incubated with or without the indicated concentration of PAC_1/$VPAC_2$ receptor antagonist, PACAP 6-38 (n = 3, PACAP6-38 5 μM **P = 0.0027, 10 μM ***P = 0.00045 compared with PACAP stimulation alone) and (C) pretreatment of either ERK or p38 inhibitor (n = 3, PACAP stimulation alone **P = 0.0012, SB202190 ***P = 0.0008, ##P = 0.005, PD98059 *P = 0.018, #P = 0.0018, SB202190 & PD98059 #P = 0.013, *compared with each control, #compared with PACAP stimulation alone). Then stathmin1 expression was quantified by real-time PCR. Data are expressed as mean ratios ±SEM relative to control values. (D) Alteration of stathmin1 mRNA levels in PC12 cells, 6 hours after PACAP or VIP treatment at the indicated concentrations, was quantified by real-time PCR. Data are expressed as mean percentages ±SEM relative to control values (n = 3, PACAP 100 nM ***P = $7.08E^{-07}$ compared with control).

doi:10.1371/journal.pone.0008596.g002

revealed that there were two types of stathmin1 containing processes; thick processes and dot-like processes. Thick processes in the granular cell layer could often be traced to the soma of stathmin1-positive cells (Fig. 3A, B). Numerous dot-like processes were exclusively found in the polymorphic layer and often formed varicosities (Fig. 4A, B white arrows). Immunoelectron microscopy established that stathmin1 positive cells extend neurites to the hilus, and that these neurites were axons, judging by their morphology (Fig. 3D, E). Thus, the dot-like processes were the fragments of axons (Fig. 3F), while the thick processes to the granular cell layer were dendrites (Fig. 3G). Similarly, primary cultured neurons expressed stathmin1 in the soma and processes under normal conditions. MAP2 and Tau staining established that stathmin1 was expressed in dendrites (Fig. 3H, I, J) and in axons (Fig. 3K, L, M).

Elevation of stathmin1 in dentate gyrus neurons causes abnormal axonal arborization. Immunoreactivity for stathmin1 was significantly increased in the SGZ neurons of *Adcyap*$^{-/-}$ mice (Fig. 3A, B), although the actual number of immunoreactive cells was similar in mutant and wild-type mice (Fig. 3C). The number of dot-like immunoreactive fibers was significantly increased in the polymorphic layer of *Adcyap*$^{-/-}$ mice compared with wild-type mice (Fig. 4A–C). These findings show that increased expression of stathmin1 in the SGZ neurons led to pronounced arborization of the axons of SGZ neurons. Therefore, we attempted to clarify whether this *in vivo* event could be duplicated *in vitro* by using hippocampal primary cultured neurons. Over-expression of stathmin1 caused dramatic changes of axon fibers. As shown in Figure 4E and 4F, arborization of axon fibers was markedly increased by stathmin1 over-expression compared with that in normal primary cultured neurons (Fig. 4D). The number of secondly neurites from axons was also increased following over-expression of stathmin1 (Fig. 4G). Thus, it was concluded that an increase of stathmin1 expression in SGZ neurons leads to abnormal axonal arborization.

Molecular mechanism of stathmin1 regulation by PACAP

PACAP regulates stathmin1 expression via the PAC_1 receptor in SGZ neurons. If PACAP directly regulates stathmin1 expression *in vivo*, SGZ neurons should express PAC_1. In fact, strong expression of PAC_1 mRNA was identified throughout the entire granule cell layer, including the SGZ (Fig. 5A). Figure 5C shows the localization of stathmin1-expressing neurons (brown) and PAC_1 mRNA-expressing neurons (black grains) in the same section of the dentate gyrus. As indicated by